 https://doi.org/10.18171/1.093101

RefTide: The Reflection and Resonance Behaviour of Tide Dominated Estuaries

Vanessa Sohrt[1], Sebastian S. V. Hein[2], Edgar Nehlsen[3], Thomas Strotmann[4] and Peter Fröhle[3]

[1]Technische Universität Hamburg, Institut für Wasserbau, vanessa.sohrt@tuhh.de
[2]Hamburg Port Authority, Abteilung Hydrologie, sebastian.hein@hpa.hamburg.de
[3]Technische Universität Hamburg, Institut für Wasserbau
[4]Hamburg Port Authority, Abteilung Hydrologie

Summary

Tidal waves entering estuaries are amplified or attenuated due to processes resulting from cross-sectional convergence, friction, reflection and resonance. While there is a basic understanding of the processes of reflection and resonance of tidal waves, there is a knowledge gap in the quantification of the processes for tidal waves in estuaries and especially of the effects of multiple reflections and re-reflections. Within the BMBF-funded KFKI-research project RefTide these gaps have been addressed with the aim to improve the system and process understanding of reflection and resonance in tide dominated estuaries. The Elbe estuary was chosen as the study area. In RefTide a comprehensive analysis of the tidal dynamics of the Elbe estuary (and the influence of different factors on the tide generated oscillations) is carried out by combining advanced analytical and numerical models with empirical studies based on available time series of water level and flow data. In addition, in RefTide methods for resonance analysis were (further) developed and applied to the Elbe estuary.

The reflection behaviour of tidal waves was investigated model-based using a self-developed analytical model as well as on a large number of model tests with different hydrodynamic numerical models (principal models, Elbe estuary model).

The results of the investigations improve the knowledge on the formation of the tide generated oscillatory system and clarify the importance of reflection, resonance and dissipation of tidal waves in estuaries. In addition, the effects of various influencing factors on the oscillatory system were determined and described. Resonance is a consequence of reflection and represents the formation of a standing oscillatory system in which, as a result of a maximum possible constructive superposition at the reflector, the largest possible amplitudes related to the amplitudes at the entrance to the system of a wave occurs. This condition has not been reached in the Elbe estuary so far. However, there are signs that the resonance case is being approached.

The following contribution presents selected key parts of the research results from the RefTide project. A detailed version of the final report (Hamburg Port Authority and Technische Universität Hamburg 2022) is available from the Leibniz Information Centre for Science and Technology University Library.

Received 13. September 2022, Reviewed 11. November 2023, Revised 21. April 2023, Accepted 23. April 2023, Available online 08. May 2023

Keywords

Elbe, eigenfrequency, eigenperiod, estuary, partial tide, tidal constituents, reflector, reflection, re-reflection, resonance, standing wave, tidal range, tide

Zusammenfassung

Tidewellen, die in Ästuare einlaufen, werden als Folge der Querschnittskonvergenz oder als Folge von Prozessen wie Reibung und Reflexion verstärkt oder abgeschwächt. Während es ein grundlegendes Verständnis zum Ablauf der Prozesse Reflexion und Resonanz von Tidewellen gibt, bestehen weiterhin Wissenslücken bei der Quantifizierung der Prozesse für Tidewellen in Ästuaren und insbesondere bei der Quantifizierung der Wirkung von mehreren Reflexionen in Kombination mit Re-Reflexionen. Im Rahmen des vom BMBF geförderten KFKI-Forschungsvorhabens RefTide wurden diese Lücken angegangen mit dem Ziel, das System- und Prozessverständnis von Reflexion und Resonanz in tidedominierten Ästuaren insgesamt zu verbessern. Als Untersuchungsgebiet wurde das Elbeästuar gewählt. In RefTide wird eine umfassende Analyse der Tidedynamik des Elbeästuars (und des Einflusses verschiedener Faktoren auf die tidebedingten Schwingungen) auf der Grundlage analytischer und numerischer Modelle sowie empirischer Untersuchungen auf der Grundlage verfügbarer Wasserstands- und Strömungsdaten durchgeführt. Darüber hinaus wurden in RefTide Methoden zur Resonanzanalyse (weiter-)entwickelt und auf das Elbeästuar angewendet.

Die Detailanalyse der Einflüsse auf das Reflexionsverhalten von Tidewellen in Ästuaren wurde mit einem weiterentwickelten analytischen Modell sowie mittels einer Vielzahl von Modelluntersuchungen mit verschiedenen hydrodynamisch-numerischen Modellen (Prinzipmodelle, Elbeästuarmodell) durchgeführt.

Die Ergebnisse der Untersuchungen verbessern die Kenntnisse über die Entstehung des tidegenerierten Schwingungssystems und verdeutlichen die Bedeutung der Reflexion, Resonanz und Dissipation von Tidewellen in Ästuaren. Darüber hinaus wurden die Auswirkungen verschiedener Einflussfaktoren auf das Schwingungssystem erfasst und beschrieben. Resonanz ist eine Folge der Reflexion und stellt die Ausbildung eines stehenden Schwingungssystems dar, in dem durch eine maximal mögliche konstruktive Überlagerung am Reflektor die größtmöglichen Amplituden bezogen auf die Amplituden am Eingang des Systems einer Welle auftreten. Diese Bedingung ist im Elbeästuar bisher nicht erreicht worden. Es gibt jedoch Anzeichen für eine Annäherung an den Resonanzfall.

Der folgende Beitrag stellt ausgewählte Kernbestandteile der Forschungsergebnisse aus dem RefTide-Projekt vor. Eine ausführliche Fassung des Abschlussberichts (Hamburg Port Authority and Technische Universität Hamburg 2022) ist in der Universitätsbibliothek des Leibniz-Informationszentrums für Technik und Naturwissenschaft erhältlich.

Schlagwörter

Ästuar, Eigenfrequenz, Eigenperiode, Elbe, Gezeiten, Partialtiden, Reflektor, Reflexion, Re-Reflexion, Resonanz, stehende Welle, Tidehub, Tide

1 Introduction

Tidal waves are altered as they pass along an estuary. They may be amplified or attenuated due to processes such as cross-sectional convergence, dissipation, wave-wave interactions and reflection. Standing tidal waves may occur in an estuary due to the reflection of tidal

waves at reflectors such as abrupt changes of width and/or depth. In some estuaries the run-up length of the tides is limited by a weir where the tidal waves are fully reflected back into the estuary. Resonance may occur in a reflecting tidal regime if the system length, i.e., the distance from the river mouth to a (total) reflector, is one quarter of the length of the incoming tidal wave.

There is a basic understanding of the processes of reflection and resonance of tidal waves in estuaries. However, there are knowledge gaps in the quantification of these processes especially in the interaction of reflections at multiple reflectors and re-reflectors in complex estuary systems. This is where the BMBF (Federal Ministry of Education and Research)-funded KFKI (German Coastal Engineering Research Council)-research project RefTide started. RefTide aimed to improve the system and process understanding of reflection and resonance in tide influenced estuaries using the Elbe estuary as an example. The Elbe estuary was chosen as study area because of the high data availability: For the analyses, 25 gauges were considered, which have been providing continuous digital measurement series with a temporal resolution of one minute since November 1999. The spatial resolution is on average one gauge every 7 km over a total length of 170 km from the mouth to the weir.

Within the research project RefTide, a comprehensive analysis of the tidal dynamics of the Elbe estuary was carried out by combining advanced analytical and numerical models in combination with an extensive analysis of the tides and partial tides (also known as tidal constituents) that finally form the measured water levels and the corresponding flow conditions (in detail described in chapter 3.3). The tide-generated oscillations as well as the influence of different factors (e.g.: tidal range, mean water level, river discharge, water volume of the Elbe estuary, bottom roughness) on the oscillation system were investigated by empirical studies using measured water level and flow data. Methods for resonance analysis were developed and applied to the Elbe estuary. The reflection behaviour of tidal waves was investigated model-based using a self-developed analytical model as well as a large number of hydrodynamic-numerical model tests with different models such as several principal models and a comprehensive Elbe estuary model.

Existing analytical models are mainly based on the method of damped co-oscillating tides and have been developed e.g., by Hunt (1964), Ippen and Harleman (1966), Marche and Partenscky (1972) or Hartwig (2016). They include the basic interrelations but are system-inherently based on strong simplifications in the geometry, the physical processes taken into account or the limited (only one) number of reflectors. These general analytical models were improved by including multiple reflectors, Elbe-specific system parameters and their variations.

There is only limited research on the analysis of reflection and resonance in estuaries. In Hensen (1941) the process of reflection of a tidal wave was described: It illustrates that the reflected wave propagates in the opposite direction of the incoming wave. The proportion of the reflected wave in the total signal decreases with increasing distance from the reflector as a result of dissipation. Hensen (1941) also describes the reflection effect on the currents (for more details, see also chapter 2.2). Quantifications of the reflection coefficient, the effect of several reflectors as well as re-reflections are not dealt with. Díez-Minguito et al. (2012) were probably the first to conduct reflection studies on a closure of a head dam in the Guadalquivir estuary. For the analysis, a gauge method further developed by Baquerizo (1995) was used, which is based on a least square fitting technique. As a result,

a reflection coefficient of 0.4 was determined for the M_2 partial tide at the expected total reflector (head dam) instead of a reflection coefficient of 1. The deviation is probably due to the non-accounted re-reflections and the neglected dissipation in the gauge method. Eichweber and Lange (1996) wrote about the importance of reflection of higher harmonics for sediment management in the Elbe estuary. For this purpose, a spectral analysis of flow measurement data was carried out and the location of the flow minima (oscillation nodes) was compared with the location of the sites where most dredging takes place. However, quantitative statements on the reflection coefficient of the partial reflectors are missing. Hartwig (2016) investigated the oscillation behaviour of the tidal wave in the Elbe. The investigations are based on the one hand on an analytical model (one reflector, linear dissipation term) and on the other hand on a numerical model ("Vector-Ocean Model Shallow Water 2-dimensional"). By experimentally estimating the damping ratios and wavelengths to approximate the equations of the analytical model to the measured data, a reflection coefficient of 18 % was determined for river kilometre 617 (location of the maximum tidal range). Resonance investigations were carried out with the numerical model. It was found that since 1970 the natural period of the Tidal Elbe has been reduced from 25.55 hours to 20.50 hours and that with a further approach of the excitation period by 8 hours, the Elbe estuary system is in resonance. The results allow a good comparison to the methods developed further in this publication. In detail, the project, consisting of two sub-projects, RefTide A and B, includes:

- The RefTide subproject *A: Reflection* mainly focussed on the model based analysis of the processs reflection and dissipation of tidal waves in estuaries. For this purpose, different methods of varying complexity were used, ranging from an improved analytical model to hydrodynamic numerical models.
- The RefTide Subproject *B: Resonance* concentrated on the extension of system concepts for the development of resonance in tide-dominated estuaries. The technical focus was on data processing of water level data and in the field of tool development on the harmonic analysis of partial tides using a self-developed implementation of the HAMELS method (Harmonic Analysis Method of Least Squares).

The results of the investigations explain the formation of the oscillatory system and clarify the importance of reflection and dissipation of tidal waves in estuaries and the relation between reflection and resonance.

An improved understanding of the tidal system and the governing processes is an important basis for the assessment of future developments including possible effects of climate change or adaptive management of the estuary. The project findings can already be incorporated into optimised management of the Elbe estuary, both in terms of nature conservation and fairway maintenance.

The aims of this contributions are

i) to give an insight into the research results of the project RefTide and
ii) to provide a better understanding of the reflection and resonance processes of tidal waves in estuaries, and thereby
iii) to contribute to an improved understanding of tides in estuaries, with a spatial focus on the Elbe estuary.

In chapter 2 of this paper, the theoretical basics of a) tidal waves, which are dominant in the Elbe estuary, b) the reflection of tidal waves and c) tidal resonance are presented. Chapter 3 presents materials and methods. Chapter 4 contains the results from the reflection analyses, the evaluations and analyses of the measurement and simulation data showing the tidal oscillation system and the results from the resonance analyses. Chapter 5 summarises the conclusions that can be drawn from the research.

Obviously, not all research results from the research project RefTide can be included in such kind of overview-contribution. A detailed final RefTide-report (Hamburg Port Authority and Technische Universität Hamburg 2022) is available from the Leibniz Information Centre for Science and Technology University Library. Additionally, parts of the results have already been published in Sohrt et al. (2021) and Hein et al. (2021).

2 Theoretical background

2.1 Tidal waves

Tidal waves are gravitational waves that result from the effects of the sun and moon. The changing gravitational effects of the moon and the sun, which change relative to the rotating earth, cause a periodic movement of the sea surface (Lamb 1932, Parker 2007).

The wave periods of the principal tidal waves are larger than 12 h and, consequently, the wave lengths of tidal waves are several hundred kilometres. Tidal waves have small water level gradients so that the linear relation between the harmonic wave signals and the nonlinear influences can be neglected. Therefore, tidal waves can be superimposed from several oscillatory tidal wave components, which themselves are described by the linear wave theory as shallow water waves. Thus, the wavelengths of tidal waves are depth- and dissipation-influenced.

The equations describing the motion of tidal waves and the wave energy can be found in common coastal engineering literature, including Ippen and Harleman (1966), Dean and Dalrymple (1991), Coastal Engineering Research Center (1984) or in the recommendations of the Committee of Coastal Protection Works of HTG and DGGT (EAK) (2002).

The tides observed at a certain location can be descripted as a result of a superposition of hundreds of independent or bounded (interrelated) partial tides. According to linear wave theory, each partial tide is a harmonic wave with its own amplitude and frequency. Partial tides can be grouped based on two criteria: First, partial tides are classified according to the cause of the force into i) lunar and ii) solar main partial tides, and iii) shallow water partial tides, which describe the deformation of the tidal wave due to nonlinear shallow water mechanisms (detailed explanation in chapters 2.3.2 and 7.6 of Parker (2007)). Second, partial tides are grouped based on their frequency into long-period (e.g., MSf), diurnal (e.g., O_1), semidiurnal (e.g., M_2), and 1/x-diurnal partial tides (e.g., M_4). For a detailed description of the composition of the partial tides, see Schureman (1958) and Parker (2007).

2.2 Reflection of tidal waves

When a wave encounters an obstacle, the wave energy is partially or totally reflected. A measure of the reflectance of an incoming wave at an obstacle is given by the reflection coefficient C_r (inter alia Eagleson 1966, Coastal Engineering Research Center 1984, Goda

2000). The reflection coefficient relates the size of the reflected wave (for example, by wave height H_r or wave amplitude a_r) to the size of the incoming wave (wave height H_i or wave amplitude a_i) which results for sinusoidal waves in:

$$C_r = \frac{H_r}{H_i} = \frac{a_r}{a_i} \tag{1}$$

A reflection coefficient $C_r = 0$ means that no reflection occurs. If the reflection coefficient is $C_r = 1$, a total reflection occurs, i.e., 100 % of the wave energy is reflected at the obstacle. If the reflection coefficient is $0 < C_r < 1$, only parts of the incoming wave energy are reflected and other parts of the wave energy are transmitted. The transmission coefficient is defined as the ratio of the size of the transmitted wave to the incoming wave.

For tidal waves, reflectors are not only hydraulic structures such as weirs, which are frontally encountered by the tidal wave, but also abrupt changes in cross-section that may occur due to changes in water depth or width, for example, at islands or harbour basins. The derivation of the reflection coefficient for long-period waves via the balance of wave energies under the assumption of continuity of the pressure and water surface can be found in Sohrt et al. (2021). The reflection coefficient C_r is:

$$C_r = \frac{1-\frac{b_2}{b_1}\cdot\frac{\sqrt{h_2}}{\sqrt{h_1}}}{1+\frac{b_2}{b_1}\cdot\frac{\sqrt{h_2}}{\sqrt{h_1}}} \tag{2}$$

where h are the water depths and b are the widths at locations 1 (downstream of the partial reflector) and 2 (upstream of the partial reflector). The transmission coefficient C_t is:

$$C_t = \frac{2}{1+\frac{b_2}{b_1}\cdot\frac{\sqrt{h_2}}{\sqrt{h_1}}} \tag{3}$$

Where Eq. (3) is only valid for $a_i \cdot C_t < h_2$ (wave height has to be smaller than water depth).

Waves do not only reflect at cross-sectional constrictions (i.e., $h_1 > h_2$ or $b_1 > b_2$), but also at cross-sectional expansions (i.e. ($h_1 < h_2$ or $b_1 < b_2$). In this case, however, a partial reflection with a phase shift of 180° occurs. Figure 1 visualises the partial reflection process for a cross-section narrowing and a cross-section widening at an abrupt bathymetric change (bottom step) over the location. Along the location, the incoming (black), reflected (red) and transmitted (violet) wave signals are shown at different time steps. In Figure 1 b), for example, it can be seen at the time step $t = t_1$ that a destructive superposition with a minimum amplitude of the resulting signal (blue) is formed when the incoming and reflected waves are 180° out of phase. The transmitted wave has a larger amplitude due to the cross-sectional constriction (left) than due to a cross-sectional expansion (right). In Figure 1 e) the phases approach nearly phase equality; in which case the maximum amplitude of the resulting signal occurs (constructive superposition). The above quantities for the reflection and transmission coefficients derived from conservation of energy are consistent with the analytical equations from Lamb (1932) and Dean and Dalrymple (1991), who calculated the reflection and transmission coefficients of long period waves at abrupt bathymetric changes via a continuity of mass fluxes.

 https://doi.org/10.18171/1.093101

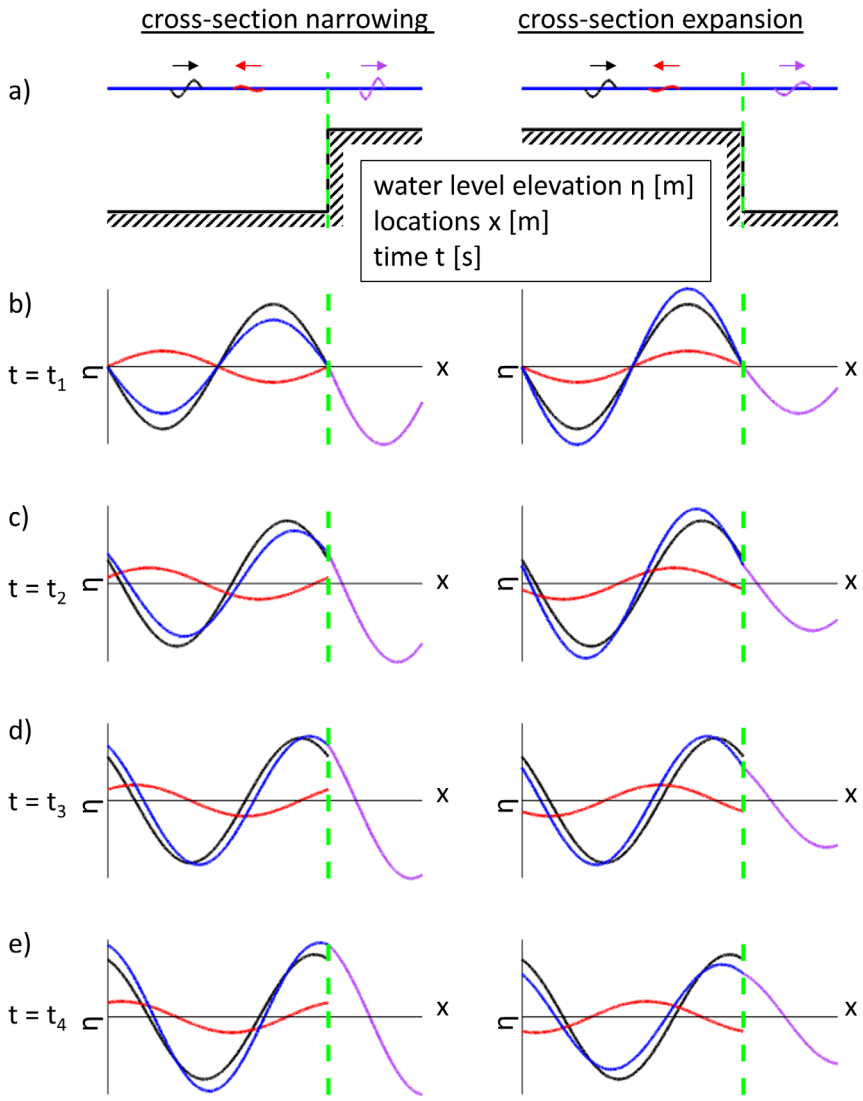

Figure 1: Illustration of the partial reflection process for an abrupt bathymetric change (bottom step) (a) along the location x at different time steps t (b-e). The resulting wave (blue) is composed of the incoming (black) and reflected (red) wave. On the other side of the reflector, the wave is transmitted (violet).

Figure 2 illustrates the process of a partial reflection (temporal representation at different locations). In Figure 2 a) the incoming, reflected and transmitted wave is shown along the longitudinal section with an abrupt bathymetric change (partial reflector). In sections b) and c) the hydrographs (water level elevations and velocities) are shown at different locations 1 to 4, which are marked in panel d) and e). When comparing the extreme values of the comprehensive signal (blue) with the positions of the slack water points (green), it becomes visible, especially in the case of locations that are out of phase with each other (see location 2), that the positions of the slack water points are shifted by the partial reflection from the maxima of the water level elevations. If the incoming signal is in phase (or 180° out of phase) with the reflected signal (e.g., location 3), the positions of the slack water points are at the extremes of the comprehensive signal. In sections d) and e) the maxima of the water level elevations and velocities of the resulting signal are shown (partially standing wave). The partially standing wave of the flow velocities are opposed to that of the water level elevation (oscillation node (amplitude minima) and antinode (amplitude maxima)

positions reversed). Thus, the lowest maximum flow velocities occur in the area of the oscillating antinodes of the water level elevation. According to investigations by Eichweber, Lange and Rolinski (Eichweber and Lange 1996, 1998, Rolinski and Eichweber 2000), these areas of low maximum flow velocities correspond to the dredging volume maxima. In areas of antinodes of the water level elevation and thus nodes of the flow velocities, the lower flow velocities can lead to sediment accumulation and therefore necessary dredging. The maximum flow velocities inside the system increases with the maximum water level.

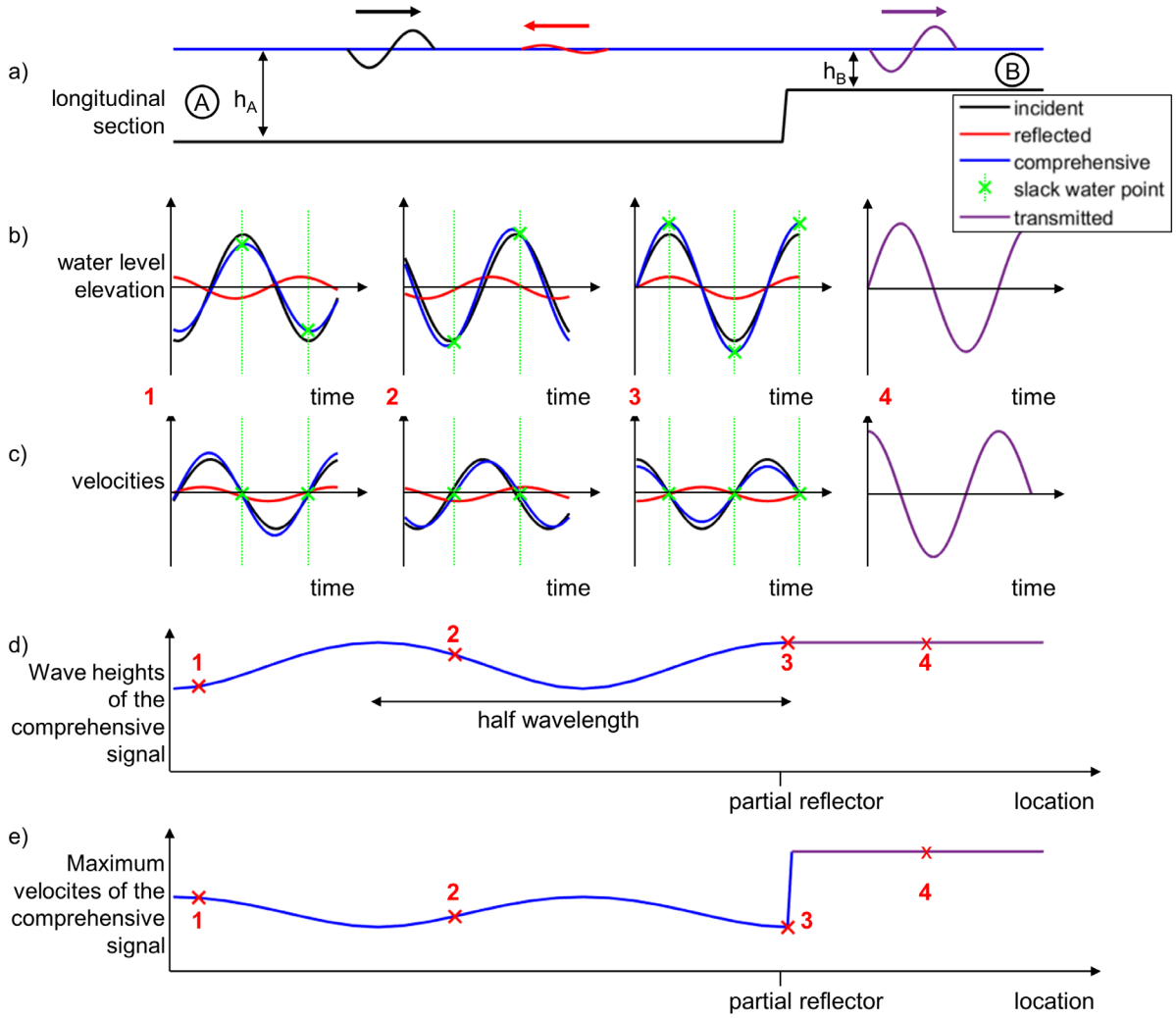

Figure 2: Simplified illustration of the reflection and transmission of a tidal wave at an abrupt bathymetric change (partial reflector). In (a) the incoming, reflected and transmitted waves at a partial reflector are shown, in (b) the water level elevations, in (c) the velocities at three different locations downstream of the abrupt bathymetric change (area A) and one location upstream of the abrupt bathymetric change (area B) are visualised. In (d) the wave heights of the comprehensive signal (partial standing wave) are shown. In (e) the maxima of the flow velocities along the longitudinal section are illustrated.

If a system contains not only one partial reflector, but several partial reflectors (e.g., R1 and R2) in combination with a total reflector (R3), a complex oscillation system is established (Figure 3): The incoming wave is reflected at the seaward reflector (reflector R1) and transmitted into the estuary. The transmitted wave encounters the next reflector (R2), where the transmitted wave is reflected and transmitted again. The part transmitted at reflector R2 is totally reflected at reflector R3 (and again reflection/transmission at R2 takes place). The

transmitted (R1) and afterwards reflected (R2) wave can again reflect at the seaward reflector (R1). From there, the reflected part of the wave remains between reflectors R1 and R2, and the other part is transmitted seaward. The thought experiment can be continued for an infinite number of reflectors as well as for an infinite number of waves that periodically enter the system again and again. Depending on whether the wave encounters a cross-sectional constriction or widening, no phase shift or a 180° phase shift of the reflected wave occurs.

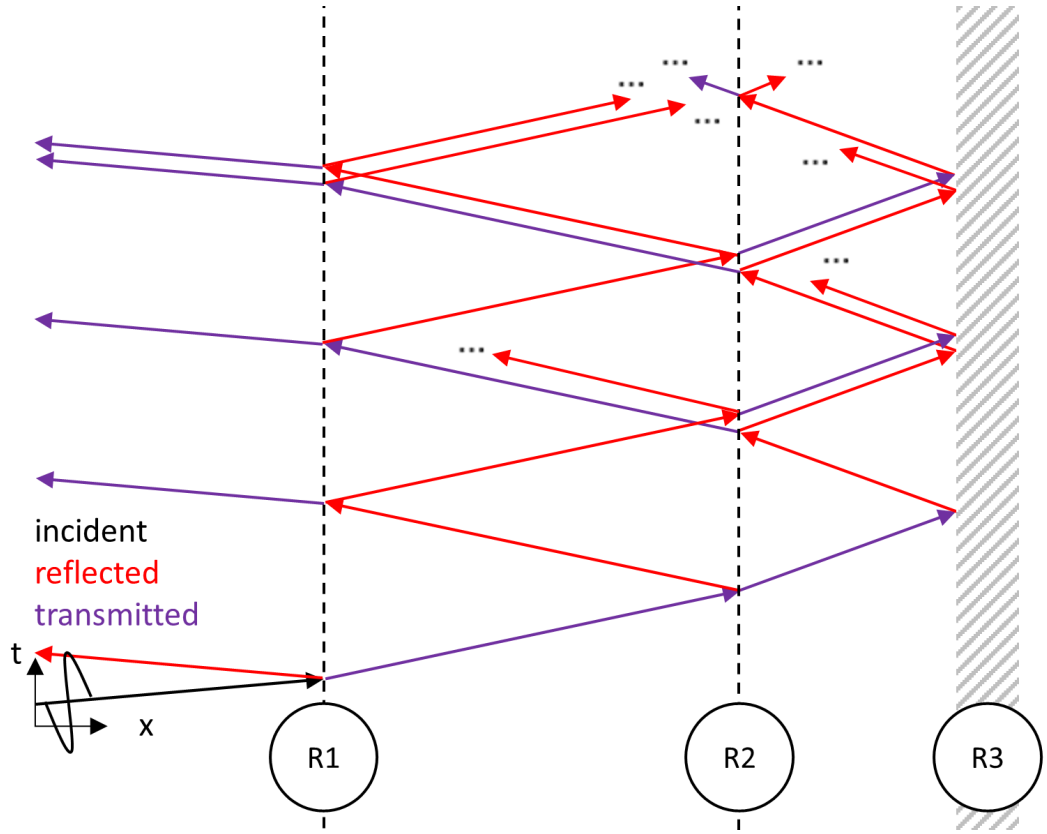

Figure 3: Overview of the incoming, reflected and transmitted wave components at two partial reflectors (R1 and R2) and one total reflector (R3).

2.3 Tidal resonance

Tidal resonance refers to a maximum constructive superposition of incoming and (re-)reflected tidal waves in an oscillatory system. Tidal resonance forms as a result of reflection for a certain system length/wavelength ratio and can be the cause of extreme tidal ranges in estuaries (as well as in bays and marginal seas). In physics, resonance is generally understood as the amplified co-oscillation of an oscillatory system in response to an excitation with the exciter period T_e equal to the eigenperiod T_s of the system (or an odd harmonic of this eigenperiod). The eigenperiod (also known as natural or resonance period) of a simplified undamped unilaterally closed basin/channel of constant width and depth with a total reflector at its closed end depends on its length l and the wave speed c (Harris 1894). In shallow waters c is equal to the square root of the product of the gravitational acceleration g and the water depth h:

$$T_s = \frac{4l}{\sqrt{g \cdot h}} \tag{4}$$

The period T_e of a wave acting as an exciter with a wavelength L can be calculated as follows (e.g. Harris 1894):

$$T_e = \frac{L}{\sqrt{g \cdot h}} \quad (5)$$

In the case of tidal waves, however, the period is astronomically determined, so only the tidal wavelength can vary with depth. From the formulae (4) and (5) it can be seen that the exciter period and eigenperiod are equal and resonance occurs if the length of the basin is a quarter of the tidal wavelength, which is also known as the quarter-wavelength criterion (further explained in, e.g., Proudman (1953)). In the case of free-end reflection, the nodes of oscillation of a resulting standing wave are located at a distance $n/4\,;\ n \in 2\mathbb{N}+1$ of the wavelength away from the reflector. Consequently, if the quarter wavelength criterion is fulfilled the wave has travelled half a wavelength after half the wave period when it reaches the mouth after reflection at the closed end, which corresponds to the distance between the wave trough and the wave crest. Thus, the wave trough of the incoming tidal wave and the wave crest of the already reflected wave meet simultaneously at the mouth and destructively superimpose to zero, which is called an oscillation node. The eigenoscillation of the system and the forced exciter oscillation are synchronous in the resonance case. The eigenoscillation and the exciter oscillation thus act simultaneously in the same direction on the water level elevation at the reflector and constructively superimpose on each other, increasing the amplitude. Thus, due to resonance, the absolute amplitude in the oscillation system is increased and the amplification within the estuary, i.e., the ratio of the amplitude at the closed end relative to the amplitude at the open end, approaches infinity, as the amplitude in the oscillation node at the river mouth approaches zero (Figure 4). This applies not only to the ratio of the wavelength to the system length of ¼, but also to odd multiples of this ratio, whereby the exciter period corresponds to an odd harmonic of the eigenperiod.

Furthermore, the oscillation system does not behave in a binary manner, i.e., there are not only the states of fully established resonance with maximum constructive superposition and no resonance. Rather, the amplitude in the oscillation antinode at the closed end and the amplification inside the system increases smoothly as the quarter-wavelength criterion is approached. In this context, shortening and deepening the estuary increases the eigenfrequency, with the shortening having the greater effect. The state of such amplified but not yet maximally constructive superposition shall be called "latent resonance", after Backhaus (2015), who defined the term for the resonance case that is not fully developed but potential, so that the tidal oscillation is already elevated. If friction occurs in the system, not a pure standing wave but a partial standing wave arises, i.e., the superposition of a standing wave and a progressive wave, whose proportion of standing wave decreases with increasing friction and distance to the reflector. The amplitude in the "quasinode" is then non-zero, but only minimal due to maximum destructive superposition of incoming and (re-)reflected waves, which can be additionally changed by the presence of further reflectors. Since friction also modifies the wave speed and thus the wavelength due to the astronomically fixed period, the tidal wavelength shortens with increasing friction and the oscillation node moves towards the closed end, also affecting the system length to wavelength ratio.

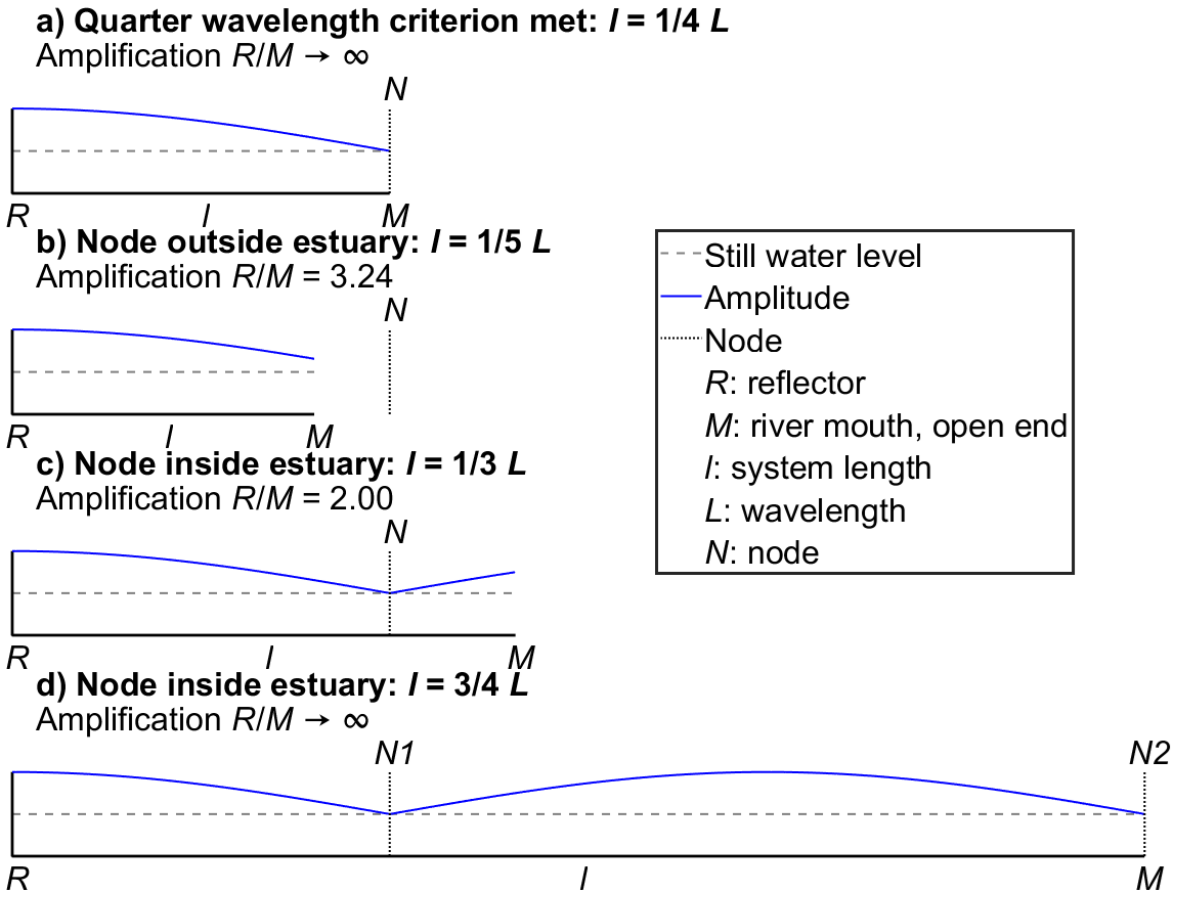

Figure 4: Schematic representation of the quarter-wavelength criterion with formation of the typical standing waves at different ratios of the system length *l* to the tidal wavelength *L*, including the tidal wave amplification between the reflector at the closed end *R* and the river mouth (open end) *M*.

3 Material and methods

3.1 Study site

The Elbe estuary has already been adequately described in the literature, e.g., in Boehlich and Strotmann (2008), Hein et al. (2021) or in Wasserstraßen- und Schifffahrtsverwaltung des Bundes (2022), to which we refer. Figure 5 shows the bathymetry of the Elbe estuary including the gauge stations in the Elbe and the river kilometres. The smaller figure in the lower left corner represents a longitudinal cross section through the bathymetry data along the Elbe estuary navigation channel. The location of the partial reflectors around the Elbe-km 710 at the mouth of the estuary and around Elbe-km 620 in the harbour area of Hamburg can be identified. Since the partial reflectors have a certain length, these are indicated by the red dotted areas. At Elbe-km 586 is the weir in Geesthacht, built in the 1960s, which represents the tidal limit and the total reflector.

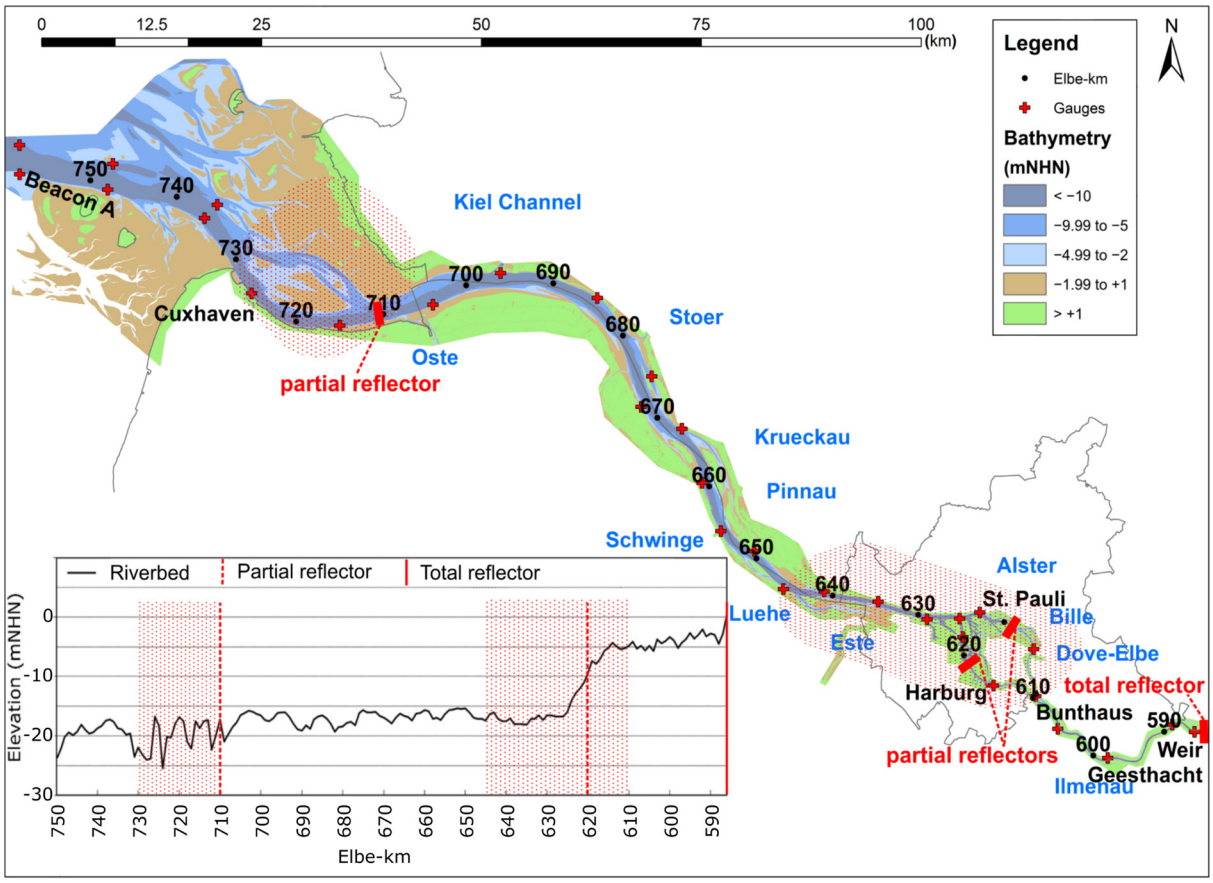

Figure 5: Overview of the Elbe estuary. Bathymetry data after the digital terrain model of the water course DGM-W-2016 with the location of the reflectors (red dotted areas). Additionally shown is the fairway bathymetry averaged over 1 km representative for the investigation period. Modified after Hein et al. (2021).

3.2 Data

The water level data from the tide gauges in the Elbe estuary and from the island of Helgoland in the German Bight are available on the ZDM website of the Federal Waterways and Shipping Administration (WSV) at www.kuestendaten.de. The temporal resolution of the hydrographs is 1 min. The tide gauge data were checked for plausibility by the Hamburg Port Authority (HPA). In the process, shorter data gaps (up to 120 min) were supplemented by means of polynomial splines and longer data gaps by means of a three-gauges correlation with the hydrographs of available neighbouring gauges shifted by the respective travel time. Spikes are corrected by low-pass filtering (cut-off frequency: 1/30 min) in the frequency spectrum of the time series. Digital time series are available for the gauges on the Elbe estuary starting with the hydrographical year 1998, with the exception of the gauges in the administrative area of the WSA Lauenburg (Elbe estuary upstream Hamburg) starting one year later. A longer data gap of almost two years (2012–13), which could not be closed, exists at the Otterndorf gauge.

For the analyses of the flow velocities, data from the HPA's permanent measuring station Nienstedten/Teufelsbrück (Elbe-km 630.8) and the permanent flow measuring stations D1 (Elbe-km 643.0), D2 (Elbe-km 651.32), D3 (Elbe-km 664.67) and D4 (Elbe-km 676.46) of the WSV were taken into account. The WSV flow measuring stations deliver

near-surface flow data every five minutes. The HPA measuring station measures the mean flow over a horizontal cross profile at a height of −4.6 m NHN every minute.

The mean daily river discharge into the Elbe estuary is measured at the gauge Neu Darchau at Elbe-km 536.4, which is operated by the Waterways and Shipping Office Elbe. The discharges measured here reach the Hamburg port area about one day later, whereby larger river discharges arrive with a shorter delay. No significant inflows into the Elbe occur between Neu Darchau and the Elbe estuary.

The bathymetric data (digital terrain elevation models of the watercourse, German abbreviation: DGM-W from the years 2010 and 2016) originate from the Coastal Data Portal of the WSV, accessed via www.kuestendaten.de. In addition, the WSV made fairway and total riverbed sounding data available to the project partners.

3.3 Methods

3.3.1 Analytical model

The analytical model (RT-A: RefTide-Analytical) developed in the RefTide project and more described in the final RefTide-report is used for the parameterized calculation of the oscillation system of the tide in estuaries; in addition, it is able to quantify the reflection coefficient of tidal waves at partial reflectors as a result of, for example, abrupt cross-sectional changes (see Eq. (2)) and is therefore more advanced than existing analytical models (such as Marche and Partenscky (1972) or Ippen and Harleman (1966)). The analytical model RT-A for calculating the propagation of tidal waves in an estuary considers and quantifies additional reflectors and the partial reflection of several tidal waves. The basis of the analytical model RT-A is the linear wave theory in combination with Green's law to account for the convergence of the cross section, a dissipation approach for waves, and a system of equations that accounts for multiple partial reflections and total reflection. For simplicity, the cross section of the estuary is approximated to be rectangular. According to the aforementioned assumptions, the deformation of the tidal wave in the estuary as a result of nonlinearities is not considered. Furthermore, the model (like most other analytical solutions) is limited to the main component of the semidiurnal lunar tide (M_2), which is the dominating tide in the Elbe estuary. Despite the simplifications, the analytical model provides a basis for the discussion of selected aspects on the reflection and resonance behaviour of the astronomical linear tidal wave in the Elbe estuary (see chapter 4.2). For the process of reflection, the abrupt bathymetrical changes along the longitudinal section are decisive. Therefore, the analytical model is a valuable and fast calculating model for understanding the process of reflection and resonance.

3.3.2 Hydrodynamic numerical models

A hydrodynamic numerical (HN) principal model is used to investigate and evaluate the fundamental influence of different conditions on the reflection behaviour of tidal waves. For the hydrodynamic numerical simulation of flow processes the model system TELEMAC-2D is used. The computational basis of the model are the Reynolds-averaged shallow water equations (Hervouet 2000). The discretization of the space is done by the

finite element method. A computational mesh is generated for the study area and water depth and depth-averaged velocity components are computed at each node of the mesh.

The HN principal model offers the advantage that individual system parameters can be varied with otherwise constant boundary conditions and therefore statements about individual influencing factors can be derived. Furthermore, more complex geometries can be calculated with the model than with the analytical solution.

For the investigations of the reflection behaviour, a basic model (straight and unbranched channel with rectangular cross-sections) is built up (a more detailed description of the model parameters can be found in Sohrt et al. (2021)). From this basic model further submodels are derived, in which different conditions and reflectors (for example abrupt geometrical changes, islands and others) are integrated. In this model series, single or several consecutive waves of a tidal component (essentially M_2) are simulated, depending on the respective problem. Reflection and transmission coefficients are determined from the simulation results. The model results provide the basis for the results from the reflection investigations in chapter 4.1 and for the description of the influences on tidal oscillation in estuaries and the Elbe estuary in chapter 4.2.

3.3.3 Harmonic analyses

Classical harmonic analysis refers to Fourier analysis, which is also used in the form of the Fast Fourier Transform (Cooley and Tukey 1965) in the project RefTide in connection with the numerical model results (not shown here) and to determine significant partial tides for the harmonic analysis method of least squares (HAMELS). In practise of harmonic analysis of measured water levels in estuaries, the FFT is sometimes unfeasible or not purposeful, because of incomplete time series or non-constant conditions. Hence, a self-programmed HAMELS was used for the extensive spectral analyses of the tides. Non-linear analysis methods were assessed as not primarily purposeful for the project objectives and were not applied.

The developed HAMELS bears some advantages over the Fourier Transformation: Unlike the Fourier Transform, the HAMELS does not require continuous data series with equidistant time points, but can have large gaps that can be randomly distributed over the period under investigation. As the HAMELS uses multiple linear regression, the harmonic components (phases and amplitudes) of the considered partial tides are approximated to the available data. This results in the significant advantage that the data can be analysed selectively, so that phases of predefined framework conditions (river discharge, mean tidal water levels, etc.) can be selected. The self-developed further enhancements of our HAMELS offer additional advantages: The exact angular positions of all considered partial tides including their nodal corrections are calculated for each measurement time point and directly considered in the multiple linear regression. This approach increases the accuracy of the calculated amplitudes and phases, allows shorter time periods to be compared without neglecting the influence of different nodal modulations, and allows for the distinction between main and shallow water partial tides on common frequencies.

A description of the method, including the multiple linear regression and the calculation of partial tides and nodal modulations, can be found in Hein et al. (2021), chapter 4.1 of the final RefTide-report (Hamburg Port Authority and Technische Universität Hamburg 2022) and further literature, such as Schureman (1958) or Boon III and Kiley (1978).

3.3.4 Resonance analyses

For the resonance analyses, the already described quarter wavelength criterion (chapter 2.3) was applied to the Elbe estuary. Furthermore, a method was developed to determine the eigenfrequency of the oscillating system using three-parameter Lorentz curve fitting (hereafter LCF). An LCF can be used generally to determine the shape of a resonance curve (Mikhailov 2018). In freely oscillating systems, the amplification increases with the approximation between the exciter frequency and the system-specific eigenfrequency. As amplification values, the ratio of the amplitudes at the gauge Harburg at the partial reflector in the Hamburg harbour to the offshore gauge Helgoland in the German Bight is used. Accordingly, an LCF is applied over the amplification values of the partial tides to determine the eigenfrequency corresponding to the abscissa of the maximum of the fitting curve. The mathematical methodology is e.g., described in Hein et al. (2021) or more generally in Mikhailov (2018) and Betzler (2003). The considered partial tides' amplitudes were determined by applying the HAMELS to hydrographs of a full nodal cycle of 18.613 years, starting on 01.01.2000 12:00:00 UTC. No fairway adjustments took place during this period.

Furthermore, two approaches to test for the temporal development of latent resonance in the Elbe estuary were conducted. In the first approach the method of eigenfrequency estimation was used under consideration of shorter time intervals of 1616 days with a temporal offset of 3 months. The total analysis period starts with 01.01.2000 12:00 UTC and ends with 30.10.2021 23:59 UTC. In the second approach, the spatial positions of the oscillation node are considered. The oscillation node (minimum of the amplitude) of the (partially) standing wave in a one-sided open oscillation system is located at the open end (the reference point of amplification) in the case of a fully developed resonance. Therefore, the spatially positions of the hydrological years' node are used to analyse whether the oscillatory system is approaching a resonant state. To determine the oscillatory node position, a fourth-degree Fourier series curve fit was used over the annual mean tidal ranges and M_2 amplitudes of the gauges between the outer river mouth at beacon A (Elbe-km 755.6) and the oscillatory antinode at the main reflector (Elbe-km 620). In the Fourier series, a_0 is the intercept, a_i and b_i are the amplitudes of the cosine and sine functions, x is the position and ω is the fundamental frequency of the signal:

$$y = a_0 + \sum_{i=1}^{4} a_i \cos(i\omega x) + b_i \sin(i\omega x) \quad (6)$$

The slope of the regression line through the river kilometre positions plotted over the hydrological years gives the mean migration rate of the node.

The methods of determining the resonance frequency by means of the three-parameter Lorenz function as well as the nodal migration as an indicator for increasing resonance are also published in Hein et al. (2021).

4 Results and discussion

Chapter 4.1 focuses on the processes of reflection and resonance as well as their model-technical calculation. Chapter 4.2 explains the formation and the influences of the tidal oscillation system in estuaries in detail using the example of the Elbe estuary. In chapter 4.3, the resonance tests are applied to the Elbe estuary investigating the eigenfrequency of the oscillation system and the development of latent resonance.

4.1 Results from the model-based reflection analyses

Using the models and methods presented in chapter 3.3.1 and 3.3.2, reflection investigations were carried out and statements on the reflection coefficients of various reflectors were derived.

4.1.1 Reflection analyses with the analytical model RT-A

The analytical model described in chapter 3.3.1 is used to calculate the oscillation system of tidal waves under idealized conditions. It is possible to calculate the tidal waves, which are influenced by cross-sectional convergence and dissipation and are superimposed by multiple reflected signals (more information on the implementation of the model can be found in chapter 5.3 in the final RefTide-report). As an example, this publication shows the formation of the tidal oscillation system for different distances of a partial reflector to a total reflector, neglecting dissipation. The aim of this investigation is to reproduce the so-called resonance case as well as other possible oscillation conditions. In Figure 6 the violet arrows indicate the different distances from the partial reflector (green line) to the total reflector (red line). If the two reflectors are in a distance of a quarter (or an odd multiple thereof) wavelength of the exciting tidal wave, the maximum constructive superposition of the tidal waves, the so-called resonance, occurs. If the reflectors are in a distance of an even multiple of the quarter wavelength, a destructive superposition of the waves occurs (along with lower wave heights at the total reflector).

The formation of an oscillatory system is thus characterized by the ratio of the wavelength to the distance between two reflectors (Figure 6, left). In the analytical model, the cross-section ratios $b_1/b_2 = 1{,}5 \rightarrow C_r = 20\,\%$ (freely selected) are taken into account. The maximum possible overall amplitude for different distances of the partial reflector to the total reflector in relation to the wavelength are shown in Figure 6 (right) at the total reflector. In Figure 6 (right) at the violet crosses it can be seen that at a distance of a quarter of the wavelength (or an odd multiple thereof), the maximum possible constructive superposition (resonance case) is reached and it has the value $a_{ges}/a_t = 1{,}2\ \mathrm{m} \cdot 2 \cdot \sum_{n=0}^{\infty} 0{,}2^n\ /1{,}2\ \mathrm{m} = 2{,}5$ where a_t is the transmitted wave amplitude at the partial reflector and a_{ges} is the total superimposed wave amplitude. The equation is a geometric series composed of the superposition of the individual amplitudes of the transmitted and (re-)reflected wave components. The maximum destructive (subtractive) superposition of the waves occurs at half wavelength distance and is $a_{ges}/a_t = 1,2\ \mathrm{m} \cdot 2 \cdot \sum_{n=0}^{\infty}(-1)^n \cdot 0{,}2^n\ / 1{,}2\ \mathrm{m} = 1{,}66$. In this case, the first and all subsequent odd re-reflected waves destructively superimpose on the incoming wave and even re-reflected waves at the reflector. The amplitude values are each reproduced in an whole-numbered half of the wavelength. Backhaus (2015) defined the term "latent resonance" for the resonance case that is not fully developed but potential. The development towards the resonance case can be attributed to a change in dissipation if the quarter-wavelength criterion is fulfilled, and to the development of the system towards the quarter-wavelength criterion if dissipation is neglected (orange arrows).

In summary, the reflection investigations in the analytical model indicate: Even in the full resonance case, there is no infinite amplitude at the total reflector. This is due to the

asymptotic approach to zero of the amplitudes of the multiple re-reflected waves. The infinite amplification measure occurs – as also described in chapter 2.3 – through the choice of the reference point in the oscillation nodes of the standing wave. The results from the analytical model can also be confirmed by results from an HN principal model with one partial reflector and one total reflector in a distance of a quarter wavelength and excited with several tidal waves. In real estuaries (and thus also in the Elbe estuary) the tidal oscillatory system is also influenced by damping and with increased amplitude the damping also increases, which limits both the maximum amplitudes and the degree of amplification in the system.

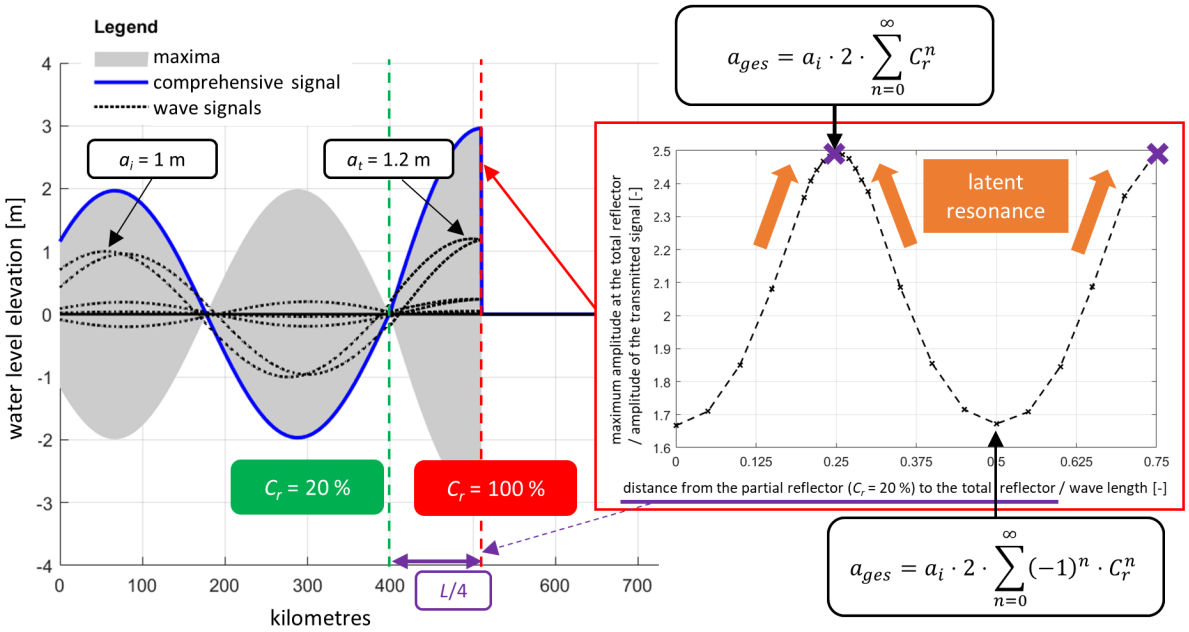

Figure 6: Results from the analytical model – variation of the distance between the partial reflector (Cr = 20 %, green) and a total reflector (red) without dissipation. Left: temporal representation of the superimposed incoming and multiple reflected components for the resonance case at the total reflector, right: variation of the maximum amplitude with different distances from the partial to the total reflector in relation to the wavelength.

4.1.2 Reflection analyses with a hydrodynamic numerical (HN) principal model

With the method described in chapter 3.3.2 it is possible to determine the main reflectors as well as their reflection coefficients. Abrupt bathymetric changes in the hydrodynamic numerical (HN) principal model were investigated as reflectors. It was found that the reflection and transmission coefficients were in good agreement with the analytical solution (Eqs. (2) and (3)) and deviations were mainly due to the model approximation of the 13.7 km long bathymetric change (bottom step) (see also Sohrt et al. (2021)). To investigate the influence of the length over which the abrupt bathymetric change extends (bottom step length), convergence tests were performed for three water depth combinations: a) h_1 = 17 m and h_2 = 6 m, b) h_1 = 9.3 m and h_2 = 4.3 m, and c) h_1 = 6 m and h_2 = 3 m – each with depth change lengths of 1 km, 5 km, 10 km, 20 km, 50 km, 100 km, 500 km, and 1000 km.

The decisive influence of the ratio value of the bottom step length to the wavelength of the partial tide as well as the good approximation of the analytical solution of the reflection

coefficient for abrupt bathymetric changes becomes clear: Figure 7 shows the ratio of the reflection coefficients from the HN simulation results and the reflection coefficients from the analytical approach against the wavelength-bottom step length ratio for the different depth combinations. The reflection coefficient depends clearly on the ratio of the wavelength of the partial tide to the length of the abrupt bathymetric change. The larger this ratio (i.e., the more "abrupt" the change), the larger the reflection coefficient becomes, approaching the analytical solution from the wave-energy-based approach (Eqs. (2) and (3)). From a ratio of the wavelength to the bottom step length of 10, all ratios of the reflection coefficients from the HN simulations to the analytical results are above 90 %. For a water depth of 17 m (water depth in the fairway downstream of Hamburg), this would be a bottom change length of over nearly 58 km. For a water depth of 9.3 m (flow cross-section-averaged effective water depth of the cross-sections in the middle Elbe estuary), the "non-abrupt" bottom change length would be over 43 km. Since the bottom change lengths in the Elbe (in the mouth area as well as in the Hamburg harbour area) are shorter than 43 km, it can be assumed that the analytical reflection coefficient is a good approximation for the abrupt bathymetric changes in the Elbe.

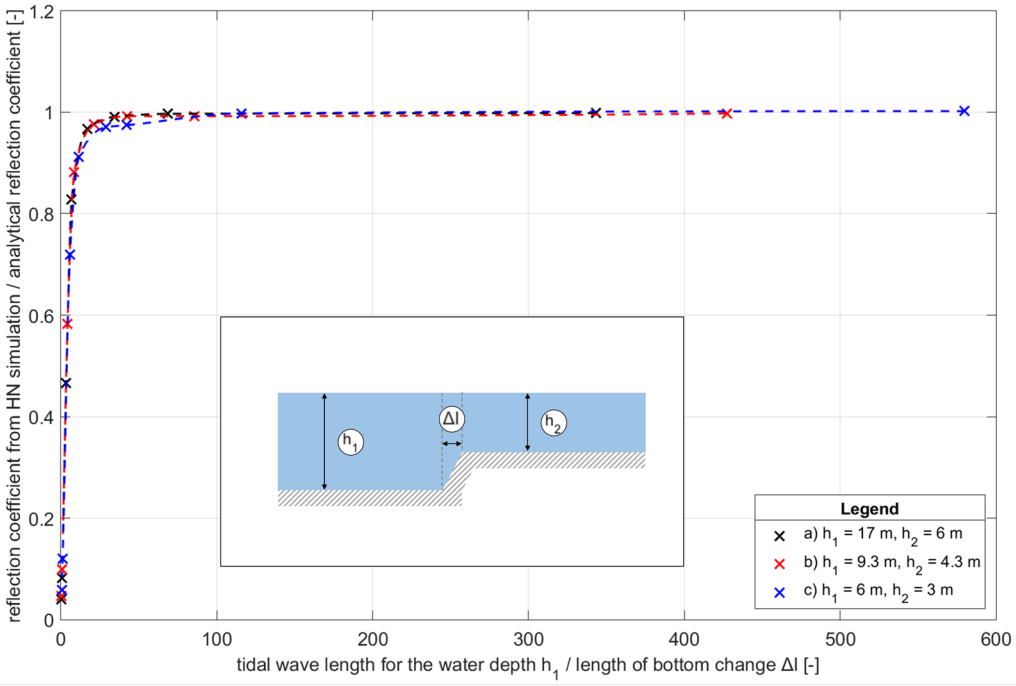

Figure 7: Ratio of reflection coefficients from simulation results and reflection coefficient from analytical approach against wavelength-bottom length ratios for various water depth combinations.

Furthermore, several abrupt changes can occur in a row, so that the cross-section is narrowed or widened over certain lengths. In this case the length over which the cross-section changes occur is important for the formation of the reflection. For this study, the cross section was constricted for a length of 500 km (Figure 8, bottom) and a tidal wave was inserted into the model (Figure 8, top, black line, $x = 0$ km). From the results shown in the top of Figure 8, it is visible that there are three clearly separable signals at $x = 1500$ km (red) generated during the simulation: First the incoming wave and second/third the reflected signals. The first signal arises from the propagation of the tidal wave along the model. The second signal comes from the reflection at the cross-section constriction (number 1, highlighted in orange) at the beginning of the island. The third signal arises from the

reflection at the cross-section widening (number 2, highlighted in blue) at the end of the island with a phase shift of 180°. The reflected signals have an amplitude of 0.33 m and 0.3 m (shown in Figure 8, top). The first reflected signal comes from the reflection at the first width narrowing by half with a reflection coefficient of 33 % ($a_r = a_i \cdot C_{r,1} = 0.33\ \mathrm{m}$). The second reflected signal comes from the transmission at the width narrowing $C_{t,1}$ = 1.33, reflection at the width widening $C_{r,2}$ = -0.33 and subsequent transmission at the cross-section widening at edge 1 $C_{t,1}$ = 0.67 ($a_r = a_i \cdot C_{t,1} \cdot C_{r,2} \cdot C_{t,1} = 0.296\ \mathrm{m}$). The first transmitted signal (number 1, blue line, x = 2500 km, highlighted in orange) is the signal transmitted at the first cross-sectional constriction ($C_{t,1}$ = 1.33) and transmitted at the second cross-sectional widening ($C_{t,2}$ = 0.67). The amplitude of the signal is found to be $a_{t,1} = a_i \cdot C_{t,1} \cdot C_{t,2} = 0.1\ \mathrm{m} \cdot 1{,}33 \cdot 0.67 = 0.089\ \mathrm{m}$, which can also be obtained from the HN simulation data. The second transmitted signal (highlighted in blue) results from transmission at the cross-sectional constriction ($C_{t,1}$ = 1.33), reflection at the second cross-sectional expansion ($C_{r,2}$ = -0.33), reflection again at the first cross-sectional expansion ($C_{r,1}$ = -0.33), and subsequent transmission at the second cross-sectional expansion ($C_{t,2}$ = 0.67). The amplitude of the signal results equivalent to 0.0097 m, which agrees with the simulation data.

If a tidal wave encounters a cross-sectional constriction and a cross-sectional widening that are located in a short distance (e.g., 10 km) behind each other, the reflected signal is superimposed in such a way that hardly any change in the water levels is formed (see Figure 72 in the final RefTide-report).

For the different factors like meanderings along the river axis, wind and river discharge no reflections of the tidal wave could be detected. However, some factors have an effect on the dissipation. For further information please refer to the chapters 5.4.2 and 5.4.3 in the final RefTide-report.

In addition to a partial reflection of a single wave, several waves can also be inserted into the model. The evaluations of an oscillation system consisting of a partial and a total reflector in the HN principal model as well as its harmonic evaluation can be read in the publication from Sohrt et al. (2021).

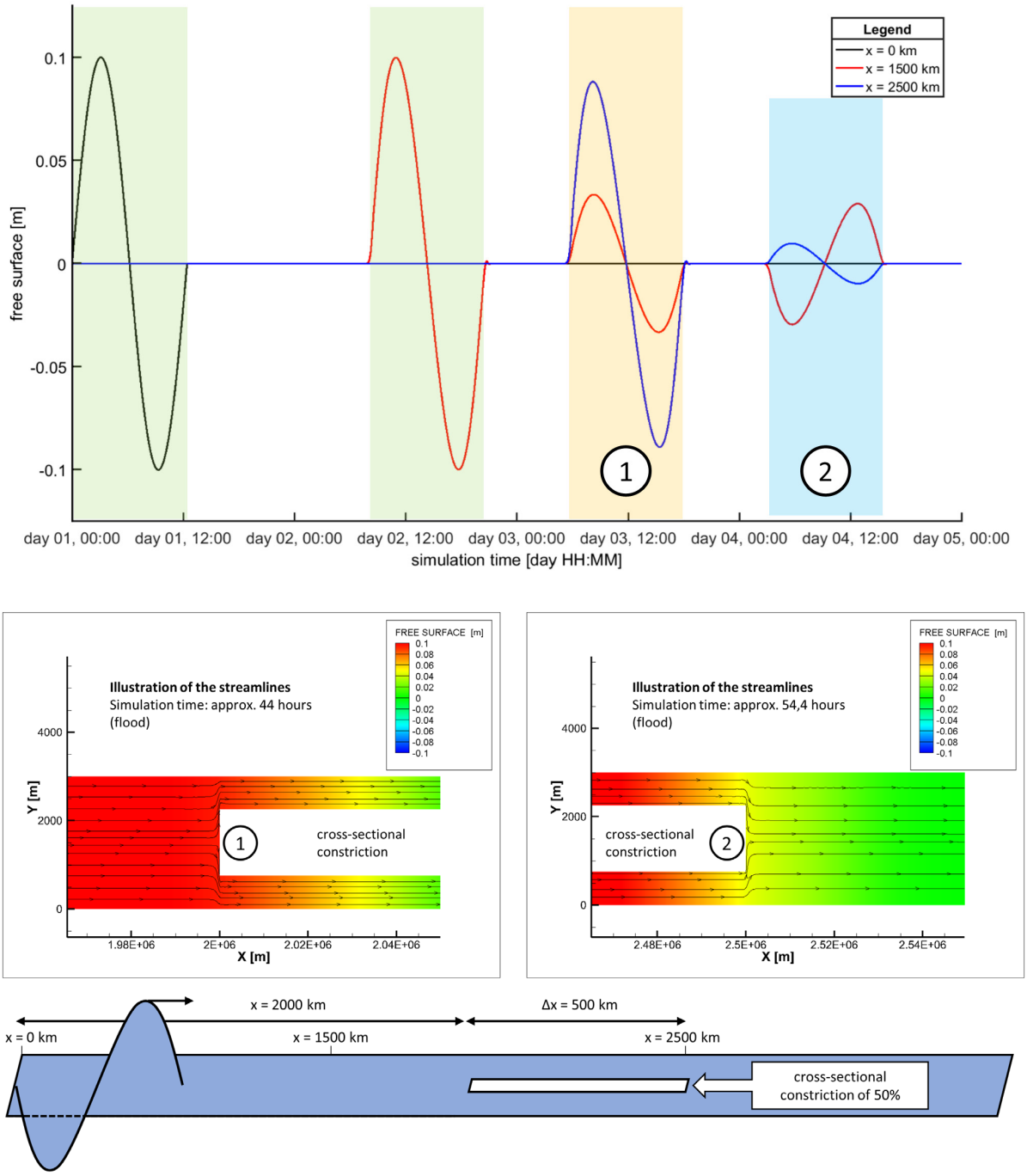

Figure 8: Representation of the HN simulation data with a 500 km long island as obstacle. Top: temporal representation of the simulation results (green background: incoming signal, yellow background: signal reflected and transmitted at cross-section constriction, blue background: signal reflected and multiply reflected and transmitted at cross-section widening). Middle: Representation of streamlines and flow around the island in the HN model. Bottom: Schematic representation of the scenario investigated.

4.1.3 Investigations with a hydrodynamic numerical (HN) Elbe model

Not only individual reflectors were investigated, but also an Elbe model calibrated and validated for mean tidal conditions (see final RefTide-report chapter 5.4.4.1) was extended downstream and upstream by one channel of constant depth each. The water depth in the

extended channels is constant 9.3 m downstream of the Elbe estuary and constant 4.3 m upstream, following the flow cross-section-averaged effective water depths of the cross-sections in the middle and upper Elbe estuary. There is no bottom friction in the model in the areas of the mesh extensions. The lower water level boundary condition is used to insert the tidal wave of an M_2 partial tide. No river discharge, wind or salinity is considered in the model for the reflection analysis.

The aim of the study is to determine the reflection coefficients of the reflectors in the Elbe estuary. Figure 9 c) gives an overview of the model used for the reflection analysis of the tidal wave. The Elbe estuary model (green box) is extended by downstream (ReflA) and downstream and upstream (ReflB) 1000 km long channels with constant width and depth each. A wave of the M_2 partial tide (green dashed wave) is inserted into these models. To be able to analyse a water level signal uninfluenced by the boundary conditions, the simulated water levels are evaluated at a distance of 900 km from the lower boundary condition (red cross in Figure 9 c). Figure 9 a) shows the total signal superimposed from the HN model at the station x = 900 km (black), which is composed of the incoming wave signal as well as several reflected and multiple re-reflected waves. Figure 9 b) shows the position of the reflectors. Reflector 1R is the partial reflector in the mouth of the Elbe estuary. Reflector 2R is the partial reflector in the Hamburg harbour area. Reflector 3R is the total reflector at the weir in Geesthacht. In Figure 9 a), the wave components from the inserted M_2 partial tide wave are assigned to the individual reflectors. The difference between the results of the simulation with the model domain ReflA (total reflector at weir Geesthacht) and the simulation with the model domain ReflB (no total reflector at weir Geesthacht) can be used to determine the time at which the signal is totally reflected at the weir (blue line in Figure 9, a, indicated with 3rd reflected wave (3R)). The water level elevations that occur from this point on are due to multiple reflections in the system of the Elbe estuary. Figure 9 a) shows both the incoming and the reflected signal into and out of the Elbe estuary model. Several wave components can be identified in the reflected signal and these can be quantified via the best fit of the harmonic wave signals to the reflected signal shown. Here, there is a possibility that there is another reflector at the Pagensander Nebenelbe in addition to the reflectors identified in the Elbe estuary (mouth of the estuary (1R), Hamburg harbour area (2R) and weir in Geesthacht (3R)). However, the reflection investigations in the HN principal model showed that with comparatively short islands in the longitudinal axis, the reflected waves are superimposed in such a way that only water level signals with a small elevation are reflected. Therefore, the reflected signal is assumed to consist of signals reflected back at only three reflectors. The deviations from the main partial tide M_2 to the simulated data result from the higher-harmonic wave components (so-called shallow water partial tides) generated during the propagation along the model. If the higher harmonics M_4 and M_6 are taken into account via the equations in chapter 7.6.2 in Parker (2007), a good agreement (RMSE: 0.005 m with an amplitude of the input signal of 0.1 m) of the wave signals with the simulation data can be achieved.

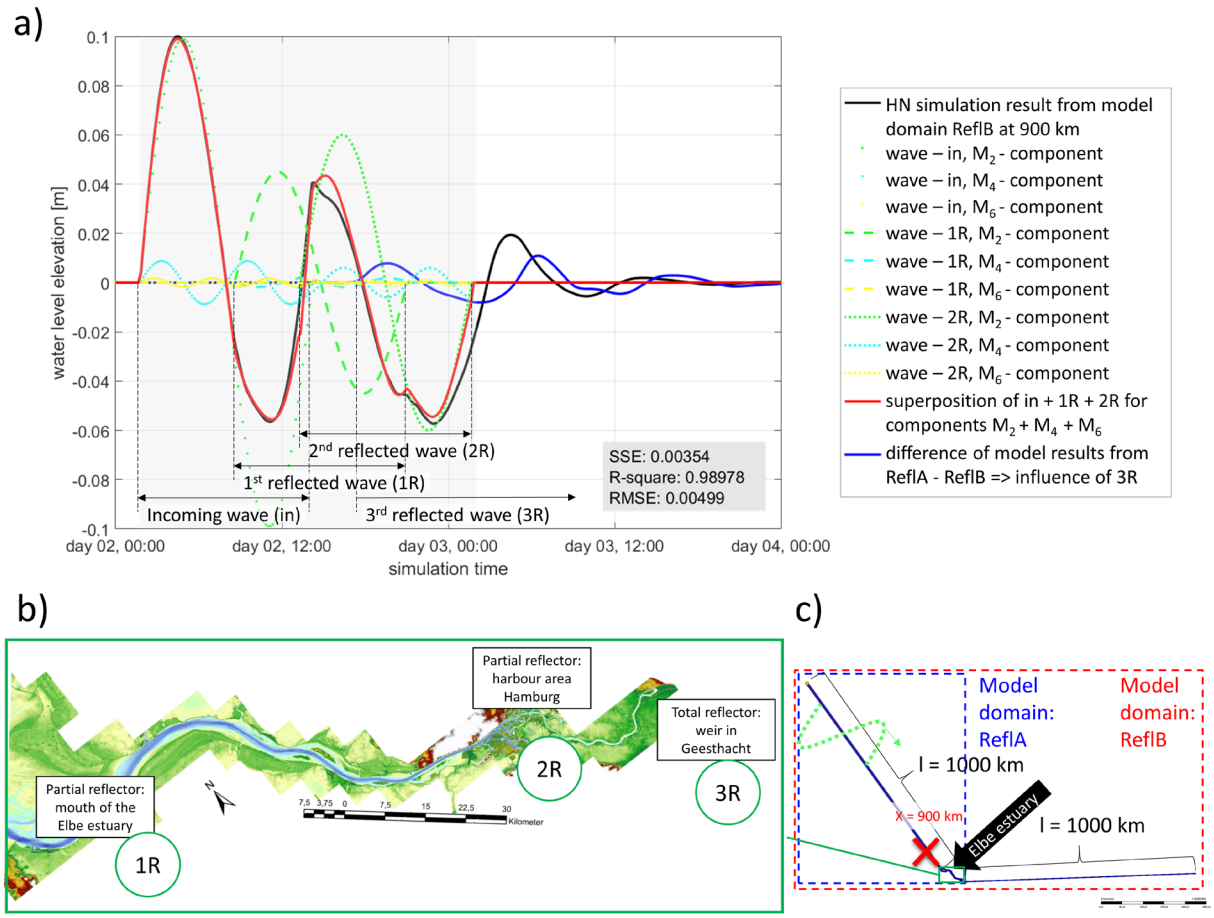

Figure 9: Results of the HN simulation for the study of tidal wave reflection behaviour in the Elbe estuary. a) Temporal representation of HN simulation result (black) compared to wave components (incoming and reflected) for different partial tide components (M_2, and its higher harmonics M_4 and M_6) at location x = 900 km (for the location see c) as well as their superposition (red), b) plan view of the Elbe estuary with the location of the reflectors (1R–3R) and c) Overview of the model domains, location of the Elbe estuary in the model and the evaluation station (X).

From the reflection analysis of the HN simulation results with the Elbe estuary model, the characteristic values listed in Table 1 for the reflectors can be derived in summary:

Table 1: Overview of reflection analysis results from the HN Elbe estuary model.

Reflector	Location of the reflector	Reflection coefficient
Mouth of the Elbe estuary	Elbe-km 710.5	~ 45 %
Bathymetric change in the Hamburg harbour area	Elbe-km 631.5	> 75 %
Weir in Geesthacht	Elbe-km 586	100 %

The reflection coefficient of the mouth in the Elbe estuary is about 45 % in the HN Elbe model. The determination of the reflectance in the Hamburg harbour area is much more complex: The signal is not analysed directly at the reflector and the reflected signal is consequently affected by influencing factors such as cross-sectional convergence, friction, the choice of input amplitude, missing river discharges and others. Therefore, no specific statement from the HN model on the reflection coefficient of the tidal wave is possible via the analysis of the reflected signal. However, if a transmission coefficient of 1.45 at the mouth

and a reversible cross-sectional convergence is assumed, the signal reflected back by 60 % relative to the incoming wave can be explained from a reflected signal with a reflection coefficient of more than 75 % (friction not considered). This reflection coefficient cannot be equated with a so-called standing wave ratio (i.e., the ratio of the height of the oscillation anti-node to the oscillation node) of the Elbe, as the oscillation system in the Elbe is influenced by multiple reflected waves and various factors as well as their complex interactions with each other.

The models serve to improve the system understanding of reflection and resonance of tidal waves. From the analysis with the simplified models, it is already possible to derive essential findings for the system of the Elbe estuary, which are summarised in chapter 5. The anthropogenic changes of the system in the past (expansion of the port of Hamburg, construction of storm surge measures, such as the weir in Geesthacht) as well as the natural morphology of the system (mouth of the Elbe estuary) determine the reflection behaviour of the tidal waves in the system. Further natural or anthropogenic changes of the system can change the reflection coefficients and thus the oscillation system of the tidal waves.

4.2 Influences on tidal oscillations in estuaries

In tide dominated estuaries, the tidal oscillation is the central factor influencing the estuarine system. Reflections are the reason for the formation of a (partially) standing oscillation system. Thus, in some estuaries or marginal seas, a tidal wave oscillatory system is evident in which an antinode and an node of oscillation can be clearly identified: Bay of Fundy in Nova Scotia, Canada (Ippen 1966, Desplanque and Mossman 2001), Gulf of California, USA (Godin 1993), Investigator Strait, South Australia (Bowers and Lennon 1990), Delaware, USA (Ippen 1966), St. Lawrence, North America (Farquharson 1962, Partenscky and Marche 1973) and many more. The Elbe also shows this characteristic tidal oscillation system. In the research project RefTide the Elbe estuary was chosen as the study area because of the high data availability and good data quality. The oscillation system in estuaries is formed due to the reflection processes described at the end of the chapter 2.2 and is additionally influenced by other factors (such as friction, river discharge, height of the mean water level, etc.) as analysed in chapters 4.3 and 6.2.1 of the final RefTide-report.

The tidal oscillation system in the Elbe estuary can be identified by harmonic analysis of the measured data. For this purpose, the further developed HAMELS described in chapter 3.3.3 was applied to the measured data and thus the tidal oscillation system was identified by the determination of the amplitudes and phases of the partial tides: The investigated diurnal, semidiurnal, quarter-diurnal and sixth-diurnal partial tides show shared frequency-group specific partial standing waves. Significantly different amplification measures can occur within the groups, for example due to shallow water partial tides. For illustrations and more detailed explanations of the identified oscillation system, see Hein et al. (2021) or the final RefTide-report (Hamburg Port Authority and Technische Universität Hamburg 2022). The same oscillation system of the M_2 partial tide could be reproduced with the HN Elbe model as well as with the analytical model (Figure 10).

In Figure 10, the M_2 partial tide components in the measured data for a river discharge class of 750 m^3/s are shown as red crosses. The results of the analytical model for the M_2 amplitude for 750 m^3/s are shown as a black line. Since the input values to the analytical

model (essentially the period of the exciting tide, cross-section values in the different sections of the lower, middle, and upper Elbe estuary, and the dissipation rates) were calibrated to these measured data, they agree very well with the oscillation system of the measured data. With the HN Elbe model (blue curve), the partial tidal components of the measured data that were derived from different time periods with the same discharge conditions cannot be reproduced exactly. This is in particular due to the choice of boundary conditions (synthetic signal from the 10 largest partial tides in the Elbe estuary, identified at the Cuxhaven station for a nodal cycle as well as a stationary river discharge of 700 m³/s, with neglect of salinity in this synthetic scenario). It is nevertheless clear that in both models, as well as from the measured data, a tidal oscillation system is clearly evident, in which the position of the nodes and anti-nodes coincide.

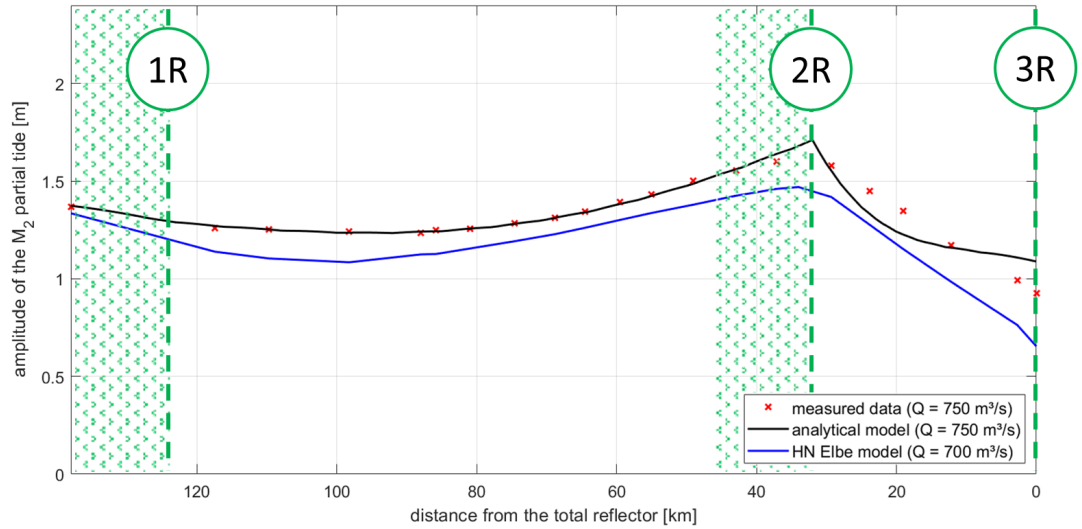

Figure 10: Comparison of the M_2 partial tide component in the analytical and numerical model results with the M_2 partial tide component in the measured data around 700 m³/s in the Elbe estuary. In reality (measured data) and in the HN model, the reflectors have a length. The areas with a green background indicate the location of the reflectors (1R: mouth of the Elbe estuary, 2R: Hamburg harbour area, 3R: weir in Geesthacht). The green dashed lines show the location of the reflectors in the analytical model.

From a series of investigations carried out with the HN principal model, it was possible to create a data basis for determining an empirical exponential function. The degree of dissipation in the empirical exponential function is dependent on different water depths, friction coefficients, specific discharges and input amplitudes. This degree of dissipation was also implemented in the analytical model and thus it was possible to make statements about a change in dissipation for different input amplitudes, water depths, roughness coefficients and specific discharges.

For the case of the Elbe this means: The area between the partial reflector in Hamburg and the total reflector at the weir in Geesthacht shows a higher degree of dissipation due to the lower water depth than downstream of Hamburg. The amplitudes of the semidiurnal partial tides are thus not doubled (or more than that due to multiple re-reflections) at the weir in Geesthacht, as it would be the case if the dissipation were neglected, but actually decrease in the direction of the total reflector. This effect can additionally be attributed to the countercurrent of the specific river discharge: the higher the countercurrent, the greater the dissipation. At high discharge classes, a decrease in the amplitudes of the semidiurnal partial tides can also be identified in the measured data. The higher-harmonic partial tides

(nonlinearities) generated as a result of shallow-water effects are not implemented in the analytical model. However, the evolution of the so-called shallow water partial tides can also be identified in the HN Elbe model: The quarter-diurnal shallow water partial tides are amplified in the area between the partial and total reflector, instead of dissipated, conforming the empirical data analyses results (presented in chapter 4.2.1 of the final RefTide-report and in Figure 3 in Hein et al. (2021)). The amplification of the quarter-diurnal shallow water partial tides is due to increased frictional influences in the upper Elbe estuary because of the stronger influence of the river discharge in combination with the shallower water depth.

4.3 Resonance analyses in the Elbe Estuary

Resonance occurs in an oscillating system when the exciter frequency is equal to the eigenfrequency (or one of its odd harmonics) of the system excited to oscillate. According to the quarter-wavelength criterion, this is the case when the system length is equal to a quarter (or an odd multiple of a quarter) of the exciter wavelength (see chapter 2.3). In addition to the quarter-wavelength criterion test, two additional approaches to test for tidal resonance were developed and applied to the Elbe estuary.

4.3.1 Quarter-wavelength criterion test

The quarter-wavelength criterion is based on simplifications (unattenuated one-sided closed channel of constant width and depth with only one total reflector at the closed end) that do not apply to any estuary. Therefore, to test for tidal resonance in oscillating systems, the quarter wavelength criterion is used as a first approach. The test for resonance is further supported by the additional approaches in the subsequent chapters.

The tidal wavelengths and system lengths of the estuary required for verification of the criterion cannot usually be determined precisely, among other things due to spatially and temporally varying conditions or the presence of multiple partial reflectors. The length of the oscillation system Elbe estuary is around 130 km (e.g. Backhaus (2015)) ±40 km, depending on chosen borders. The semidiurnal tidal wavelength in the Elbe estuary calculated using several approaches, including different effective water depths, calculated phase velocities, observed travel times and hydrodynamic numerical modelling, ranges between 300 km and 430 km (chapter 2.3.3 in the final RefTide-report). Considering the possible variation in system lengths and exciter wavelengths, the quarter-wavelength criterion can be both rejected and confirmed for the Elbe estuary. Previously published studies differ in their statement if the quarter wavelength criterion is fulfilled for the Elbe estuary: Eichweber and Lange (1998) and Rolinski and Eichweber (2000) stated that the quarter wavelength criterion is fulfilled for the Elbe estuary. Backhaus (2015) and Hartwig (2016), on the other hand, found that no full resonance is established in the Elbe estuary, but that a latent resonance occurs, which contributes to the increased tidal ranges in the port of Hamburg. However, the conducted investigations show that the node of the partial standing wave of the tidal range between 2000 and 2021 was located within the Elbe estuary between Elbe-km 685 and 699 and the node of the semidiurnal partial tide M_2 was located between Elbe-km 674 and 696 and thus not at the open end. Consequently, the quarter-wavelength criterion in the Elbe estuary is not fulfilled and no full resonance is established for the semidiurnal tides.

4.3.2 Determination of the eigenfrequency of the tidal oscillating system

Since the test of the quarter-wavelength criterion showed that the Elbe estuary is not in full resonance, i.e., the eigenfrequency is not equal to the exciter frequency of the dominant M_2 partial tide, there is a need to determine the eigenfrequency. For this purpose, the method of eigenfrequency determination via three-parameter Lorentz curve fitting (LCF) was developed. The fact that the oscillation nodes of the dominant semidiurnal partial tides are located inside the Elbe estuary indicates that the oscillation system is longer than ¼ of the dominant tidal wavelength. Consequently, it can be assumed that the eigenfrequency of the system is lower than the semidiurnal exciter frequencies. The LCF over the amplification factors (ratio of the amplitudes at the gauge Harburg at the partial reflector in the Hamburg harbour to the offshore gauge Helgoland) of the investigated diurnal and semidiurnal partial tides yields the eigenfrequency of the Elbe estuary oscillatory system of 1.5615 cycles per day (cpd) (Figure 11, left). This eigenfrequency corresponds to an eigenperiod T_s of 15.37 h. Due to the astronomically given partial tidal frequencies, there is a gap of partial tides between the diurnal and semidiurnal tides. Therefore, for further validation, an additional LCF was applied to the eighth-diurnal partial tides (Figure 11, right), in whose frequency range an odd harmonic of the eigenfrequency is located. Calculated back, this harmonic yields an eigenfrequency of 1.5424 cpd, which lies in the 95 % confidence interval [1.4961 cpd, 1.6268 cpd] of the eigenfrequency determined for the diurnal and semidiurnal partial tides.

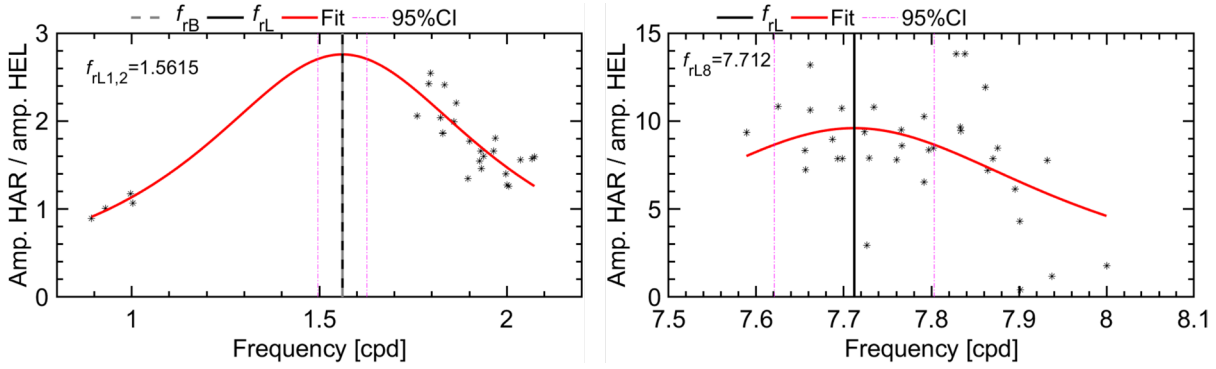

Figure 11: Determination of the eigenfrequency of the Elbe estuary via a three-parameter Lorentzian function-fit (red line). Each asterisk-marker represents the amplitude ratio for a partial tide at the respective frequency between gauge Helgoland in the German Bight and gauge Harburg at the reflector in the Southern Elbe, where maximal tidal ranges are measured. The left diagram shows the diurnal and semidiurnal partial tides. The right diagram shows the eighth-diurnal partial tides. The maximum of the fitting-functions shows the calculated resonance frequency f_{rL}. Additionally shown is the resonance frequency after Backhaus (2015) f_{rB} in the left diagram. Modified after Hein et al. (2021).

Investigations with the analytical model also showed that for the Elbe estuary certain frequencies produce a maximum amplification in the system. For the partial reflector in the port of Hamburg, the maximum amplification relative to the river mouth (factor 1.52) is reached at a frequency of 1.33 cpd, and for the total reflector at the Geesthacht at a frequency of 1.59 cpd (factor of 1.01). It should be noted that the variation of the amplification as a function of frequency decreases with proximity to the maximum and is relatively low between 1.26 cpd and 1.66 cpd. In synthesis, both the empirical data analyses and the analytical model investigations for determining the eigenperiod show that the Elbe estuary

oscillation system is not in resonance, but that the eigenperiod lies in the gap between diurnal and semidiurnal partial tides. Yet the eighth-diurnal partial tides are susceptible to resonance in the Elbe estuary but have low amplitudes in the single-digit centimetre range.

For more details and visualisations, please refer to chapter 4.4.2 in the final RefTide-report and Hein et al. (2021).

4.3.3 Indicators of increasing latent resonance

Although the investigations showed that the Elbe estuary is not in full resonance, the question arises as to whether this state is stable or whether the oscillation system changes over time. For this purpose, the development of the eigenfrequency and the oscillation node position were considered. According to equation (4), the eigenfrequency varies if the length of the estuary or its depth changes. An approach to the quarter-wavelength criterion, i.e., an approach of the eigenfrequency of the system to the astronomically determined exciter frequencies of the dominant semidiurnal partial tides, means an increase in the latent resonance and thus an approach to the fully established resonance case.

Figure 12 shows the temporal development of the eigenfrequencies determined over 1616-day intervals with a 3-month offset from 01.01.2000 to 31.10.2021. There is a decrease in eigenfrequency from the beginning of the investigation period to June 2005, which then remained constant until 2010 and then continued to decrease until 2012 to a minimum of 1.5247 cpd. This is followed by a relatively rapid increase in eigenfrequency up to 1.626 cpd by 2015 with an equally rapid subsequent decrease to a level close to the mean eigenfrequency of 1.5615 cpd. The Theil-Sen line, which does not require a normal distribution and is less influenced by outliers than a normal linear regression, shows a simplifying overall tendency for the latent resonance to increase over the study period.

The analysis of the node positions shows a seaward migration for the tidal range and for the dominant M_2 partial tide (Figure 13), which indicates an approach to a fulfilled quarter-wavelength criterion and thus increasing latent resonance. The fact, that the nodes of the tidal range are generally about 5 km to 10 km more seaward, is because the tidal range represents the envelope of all partial tides with their different node positions.

Admittedly, the development of the eigenfrequency exhibits fluctuations that entail certain uncertainties and do not speak for a constant linear development. With regard to node migration, the distances between the gauges downstream of Elbe-km 674 are, at approx. 10 km to 12 km, twice as large as in the upper part and the node positions differ between successive years, sometimes by more than 4 km. Quantitative statements about the increase in latent resonance, or node migration, must therefore be treated with caution, but the trends are clear.

As a partial cause for the increasing latent resonance, an increase of the water depths in the Elbe estuary derived from the tidal mean water rise and the water volume increase was identified. However, these cannot fully explain the increase in latent resonance. The low river discharge since 2013/14 and reduced friction (derived from the observation from Weilbeer et al. (2021)) in the Elbe estuary suggest additional causes, but their influences on the increasing latent resonance could not be clearly proven within the framework of the project.

For a more comprehensive result and discussion with additional illustrations, please refer to chapter 4.4.3, 6.2.2 and 7.2 in the final RefTide-report (Hamburg Port Authority and Technische Universität Hamburg 2022).

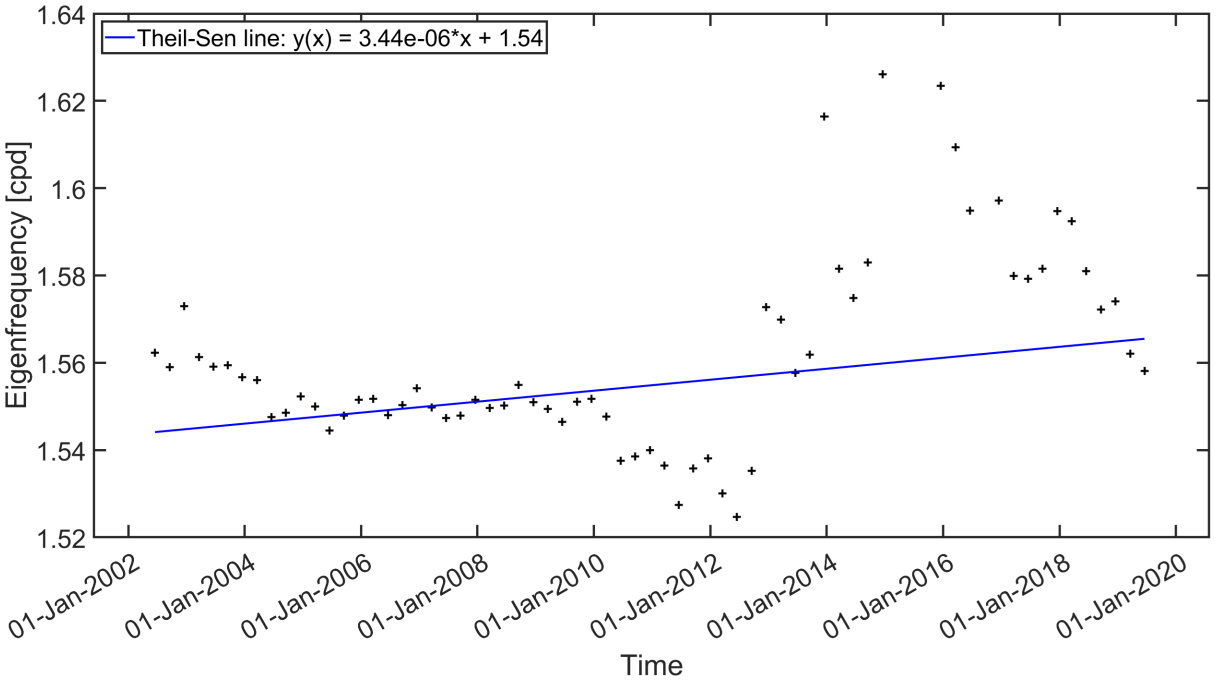

Figure 12: Eigenfrequencies of the Elbe estuary determined by Lorentz curve fitting over 1616-day intervals with a 3-month offset from 01.01.2000 to 31.10.2021. Shown in blue is the Theil-Sen line for determining the simplifying linear trend, which is robust against outliers. The function shows x in days since 01.01.2000.

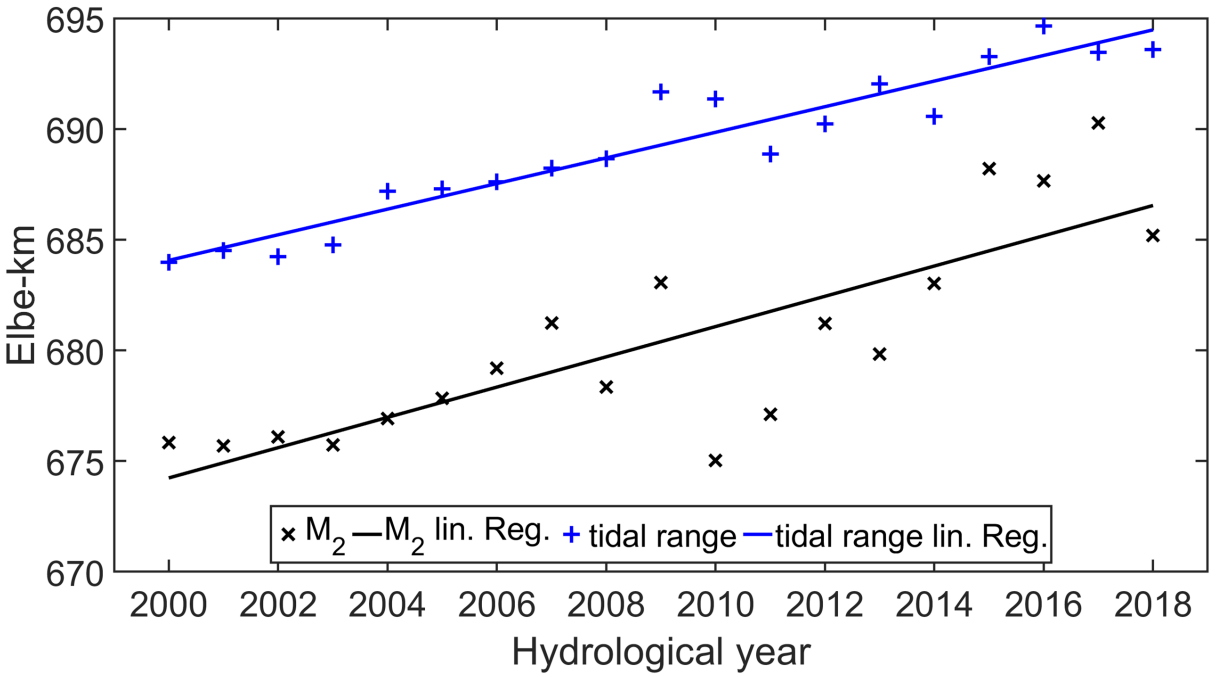

Figure 13: Oscillation node position of the M_2 (black) and the tidal range (blue) along the Elbe kilometres of the hydrological years 2000 to 2018 with corresponding linear regression lines.

5 Summary and Conclusions

The understanding of the reflection and resonance behaviour of tidal waves in estuaries in general and in particular for the Elbe estuary has been considerably improved:

- The main reflectors and their reflection coefficients for tidal waves have been determined. These include abrupt bathymetric changes (cross-sectional constrictions and cross-sectional expansions) and the total reflector at an artificial tidal boundary
  - For the Elbe estuary, these are the mouth of the Elbe estuary ($C_r \approx 45$ %), the Hamburg harbour area ($C_r > 75$ %) and the weir in Geesthacht ($C_r = 100$ %) (see chapter 4.1.3).
- In the case of two reflectors, the formation of the oscillation system depends on the distance between the reflectors to each other (chapter 4.1.1).
  - Even in the full resonance case, there is no infinite amplitude at the total reflector, but a maximum amplitude is established in the oscillation system.
  - The infinite amplification occurs due to the choice of the reference point at the open end of the system, where the oscillation node of the standing wave is located in the resonance case.
  - In real estuaries (and thus also in the Elbe estuary) the tidal oscillatory system is influenced by damping, which reduces both the maximum amplitude and the degree of amplification of the overall oscillation system.
- The reflection coefficient depends on the ratio of the wavelength of the partial tide to the length of the abrupt bathymetric change. The larger this ratio (i.e., the more "abrupt" the change), the larger the reflection coefficient becomes, approaching the analytical solution from the wave-energy-based approach (chapter 4.1.2).
- To test for tidal resonance in semi-closed oscillatory systems, new approaches have been developed. These include i) the determination of the eigenfrequency using the three-parameter Lorentzian function and ii) the detection of oscillation node migration to monitor the temporal evolution of latent resonance. These new methods were applied together with existing conventional tests to the Elbe estuary:
  - The quarter-wavelength criterion is not fulfilled, indicating that the tidal exciter frequency is not equal to the eigenfrequency of the oscillation system.
  - The eigenfrequency of the Elbe estuary was determined by the three-parameter Lorentzian function to be 1.5615 cpd (95 % CI [1.4961, 1.6268]) and thus lies in an astronomically conditioned gap between the diurnal and semidiurnal partial tides.
  - A harmonic of the eigenfrequency lies in the frequency range of the eighth-diurnal partial tides, which are thus sensitive to resonance (but their amplitudes are merely in the single-digit cm range).
  - The investigations show that the Elbe estuary is not in full resonance, but the latent resonance has increased over the investigation period, indicated by a tendentially increasing eigenfrequency and a seaward migration of the oscillation node towards the river mouth. The increase in latent resonance has contributed to the increasing tidal range in the Elbe estuary.

Further results have already been published in Sohrt et al. (2021), Hein et al. (2021) as well as in the final RefTide-report (Hamburg Port Authority and Technische Universität Hamburg 2022) and will also be presented in future publications.

The model investigations carried out show that the resonance of the tidal waves in estuaries is not linked to an infinite amplitude of the tidal oscillation – contrary to the view frequently published in the literature. If the general conditions (mean water level, river discharge, estuary geometry and roughness elements such as bed structures or the tributaries) remain the same, a stable oscillation system is established within a few tidal cycles. If the general conditions change, the oscillation system adapts to the changed conditions. Consequently, a dynamic equilibrium of the tidal oscillation system is established in the estuaries, adapted to the prevailing conditions.

The investigations of the factors influencing the oscillation system show that the general conditions were not constant during the period of investigation after the fairway adjustment in 1999, despite the absence of major river engineering measures. On the one hand, this shows that the Elbe estuary is subject to dynamic variations in the general conditions, which, in addition to anthropogenic interventions such as river engineering measures, have a significant influence on the oscillation system. On the other hand, this indicates that abrupt changes in the oscillation system can lead to persistent changes in the morphology and oscillation system even after completion. For example, a newly established oscillation system brings with it altered induced flow velocities and thus also altered sedimentary erosion and accumulation zones. In addition, such a deepening of the oscillatory system with an accompanying approach to the resonance case can set in motion an erosive process due to the increased induced flow velocities, which further deepens the system and consequently increases the latent resonance until the resonance case is fulfilled (Bakker 1998). An increasing latent resonance in the Elbe estuary can be observed over the study period. This is accompanied by increased tidal pumping. Tidal pumping describes the effect that the "asymmetry of the tide [...] causes the suspended sediment flux to be greater on the flood tide than on the ebb tide" (Dyer 1997, p. 159). With stronger flood tide the suspended sediment is pumped towards the head of the estuary und can lead to a transport of fine sediments from the mouth into the estuary (e.g. shortly explained in Brenon and Le Hir (1999)). This in turn leads to siltation of the harbour basins and the formation of fluid mud layers, which overprint the riffle and dune structures and thus reduce bed friction (discussed in Weilbeer et al. (2021)). This must be responded to by relieving the sediment balance, by exporting fine sediments from the system, while at the same time retaining the sand fraction in the system to stabilise transport bodies and consequently the entire bed. This is also necessary so that the bed roughness can be restored through the formation of new transport bodies after fairway adjustments have been carried out with the accompanying smoothing of the bed. In this context, the constantly low level of river discharge since 2014 should also be viewed critically. This leads to the fact that the fine sediment is no longer sufficiently transported out of the system and instead accumulates in the Elbe estuary. In this respect, a transnational water withdrawal management of the Elbe should be strived for, which takes into account not only regional needs but also the needs of downstream Elbe states and public interests.

The improved understanding of systems and processes is an important basis for decision-makers to estimate the effects of future developments inside the system as well as at the outer system boundaries – foreseeable also due to the consequences of climate change – and to incorporate them into adaptive action at an inter-territorial scale. Forecasts of the future development of the tidal regime in estuaries based on the knowledge gained could give new orientation to the objectives of management and development plans for nature

conservation as well as urban and port planning and coastal protection. An obvious utilisation option exists above all in the optimisation of sediment management to secure water depths in harbour entrances.

Finally, it should be emphasised that impact forecasts for future measures must also take into account possible developments over longer-term time horizons and more complex system interrelationships when planning interventions in the oscillation system such as river engineering measures. Subsequent to the measures, long-term monitoring is necessary.

6 References

Backhaus, J. O.: Latent resonance in tidal rivers, with applications to River Elbe. Journal of Marine Systems, 151, 71–78, doi:10.1016/j.jmarsys.2015.06.005, 2015.

Bakker, W. T.: Effect Resonance on Morphology of Tidal Channels. Coastal Engineering Proceedings. doi:https://doi.org/10.9753/icce.v26.%p, 1998.

Baquerizo, A.: Wave reflection on beaches: Methods of assessment and forecasting. Ph. D. Thesis, University of Cantabria. In Spanish, 1995.

Betzler, K.: Fitting in Matlab, Fachbereich Physik der Universität Osnabrück, 2003.

Boehlich, M. J.; Strotmann, T.: The Elbe Estuary. Die Küste, 74, 288–306, 2008.

Boon III, J. D.; Kiley, K. P.: Harmonic Analysis and Tidal Prediction by the Method of Least Squares: A User's Manual, 1978.

Bowers, D.; Lennon, G.: Tidal progression in a near-resonant system. A case study from South Australia. Estuarine, Coastal and Shelf Science, 30(1), 17–34, 1990.

Brenon, I.; Le Hir, P.: Modelling the turbidity maximum in the Seine estuary (France): identification of formation processes. Estuarine, Coastal and Shelf Science, 49(4), 525–544, 1999.

Coastal Engineering Research Center: Shore protection manual (4. ed.). U.S. Army Engineer Waterways Experiment Station Coastal Engineering Research Center, Washington, D.C., 1984.

Committee of Coastal Protection Works of HTG and DGGT (EAK): Die Küste. EAK 2002. Empfehlungen für die Ausführung von Küstenschutzwerken durch den Ausschuss für Küstenschutzwerke der Deutschen Gesellschaft für Geotechnik e.V. und der Hafenbautechnischen Gesellschaft e.V., 2002.

Cooley, J. W.; Tukey, J. W.: An algorithm for the machine calculation of complex Fourier series. Mathematics of computation, 19(90), 297–301, 1965.

Dean, R. G.; Dalrymple, R. A.: Water wave mechanics for engineers and scientists (Repr ed.). World Scientific, Singapore, 1991.

Desplanque, C.; Mossman, D. J.: Bay of Fundy tides. Geoscience Canada, 28(1), 1-11, 2001.

Díez-Minguito, M.; Baquerizo, A.; Ortega-Sánchez, M.; Ruiz, I.; Losada, M. A.: Tidal Wave Reflection from the Closure Dam in the Guadalquivir Estuary (Sw Spain). Coastal Engineering Proceedings, 1(33), 58, 2012.

Dyer, K. R.: Estuaries: A Physical Introduction (2nd ed.). Wiley, Chichester, 1997.

Eagleson, P.: Small amplitude wave theory. In: A. T. Ippen (Ed.), Estuary and coastline hydrodynamics 493–545, McGraw-Hill, New York, 1966.

Eichweber, G.; Lange, D.: Über die Bedeutung der Reflexion von Obertiden für die Unterhaltungsaufwendungen in der Tideelbe. Die Küste, 58, 179–198, 1996.

Eichweber, G.; Lange, D.: Tidal Subharmonics and Sediment Dynamics in the Elbe Estuary. Vortrag, 3rd International Conference on Hydro-Science and -Engineering: Brandenburg University of Technology at Cottbus, Cottbus/Berlin, 1998.

Farquharson, W.: Tides, tidal streams and currents in the Gulf of St. Lawrence. Canadian Hydrographic Service, Surveys and Mapping Branch, Department of Mines and Technical Surveys, Ottawa, 1962.

Goda, Y.: Random seas and design of maritime structures (2nd ed.). World Scientific Publishing Company, Singapore & New Jersey, 2000.

Godin, G.: On tidal resonance. Continental Shelf Research, 13(1), 89–107, 1993.

Hamburg Port Authority and Technische Universität Hamburg (Hg.): Abschlussbericht RefTide: Das Reflexions-und Resonanzverhalten Tide-dominierter Ästuare (RefTide). Eine Analyse des Antwortverhaltens der Tideelbe auf die Gezeitenanregung, Teilprojekte: Reflexion und Resonanz, Fachlicher Schlussbericht, Hamburg Port Authority, Technische Universität Hamburg, 2022.

Harris, R. A.: Seiches in lakes, bays, etc. In: Manual of tides 2, 467–482, US Government Printing Office, 1894.

Hartwig, F.: Das Schwingungsverhalten der Tideelbe hinsichtlich Resonanz. Die Küste, 84, 193–212, 2016.

Hein, S. S.; Sohrt, V.; Nehlsen, E.; Strotmann, T.; Fröhle, P.: Tidal Oscillation and Resonance in Semi-Closed Estuaries. Empirical Analyses from the Elbe Estuary, North Sea. Water, 13(6), 848, 2021.

Hensen, W.: Die Entwicklung der Fahrwasserverhältnisse in der Außenelbe. In: Jahrbuch der Hafenbautechnischen Gesellschaft 91–165, Springer, Berlin, Heidelberg, doi:10.1007/978-3-642-90884-2_10, 1941.

Hervouet, J.-M.: TELEMAC modelling system: an overview. Hydrological Processes, 14(13), 2209–2210, doi:10.1002/1099-1085(200009)14:13<2209::Aid-hyp23>3.0.Co;2-6, 2000.

Hunt, J.: Tidal oscillations in estuaries. Geophysical Journal International, 8(4), 440–455, 1964.

Ippen, A. T. (Ed.) Estuary and coastline hydrodynamics. New York: McGraw-Hill, 1966.

Ippen, A. T.; Harleman, D. R. F.: Tidal Dynamics in Estuaries. In: A. T. Ippen (Ed.), Estuary and coastline hydrodynamics 493–545, McGraw-Hill, New York, 1966.

Lamb, H.: Hydrodynamics (6. ed.). Univ. Pr, Cambridge, 1932.

Marche, C.; Partenscky, H.-W.: Deformation of Tidal Waves in Shallow Estuaries. Coastal Engineering Proceedings(13), 134–134, 1972.

Mikhailov, E. E.: Fitting and data reduction. In: Programming with MATLAB for scientists: A beginner's introduction, CRC Press, 2018.

Parker, B. B.: Tidal analysis and prediction. US Department of Commerce, Silver Spring, doi:10.25607/obp-191, 2007.

Partenscky, H.-W.; Marche, C.: Verformung von Tidewellen im Flachwasserbereich. Die Küste(24), 83–92, 1973.

Proudman, J.: Dynamical Oceanography. Methuen & Co., London, 1953.

Rolinski, S.; Eichweber, G.: Deformations of the tidal wave in the Elbe estuary and their effect on suspended particulate matter dynamics. Physics and Chemistry of the Earth, Part B: Hydrology, Oceans and Atmosphere, 25(4), 355–358, doi:10.1016/s1464-1909(00)00025-3, 2000.

Schureman, P.: Manual of harmonic analysis and prediction of tides (Vol. Special Publication No. 98). US Department of Commerce, Washington D.C., 1958.

Sohrt, V.; Hein, S. S. V.; Nehlsen, E.; Strotmann, T.; Fröhle, P.: Model Based Assessment of the Reflection Behavior of Tidal Waves at Bathymetric Changes in Estuaries. Water, 13(4), 489, 2021.

Wasserstraßen- und Schifffahrtsverwaltung des Bundes: Tideelbe – Fahrinnenanpassung 1999 – Untersuchungsrahmen. Stand 08.07.2022: https://www.kuestendaten.de/Tideelbe/DE/Projekte/FRA1999/Planfeststellungsverfahren/Antragsunterlagen/UVU/Textband/04-00-00-html.html, 2022.

Weilbeer, H.; Winterscheid, A.; Strotmann, T.; Entelmann, I.; Shaikh, S.; Vaessen, B.: Analyse der Hydrologischen und Morphologischen Entwicklungen in der Tideelbe für den Zeitraum 2013–2018, 2021.